



**HAL**  
open science

## Characterization of the *Porphyromonas gingivalis* Type IX Secretion Trans-envelope PorKLMNP Core Complex

Maxence S Vincent, Mickaël J Canestrari, Philippe Leone, Julien Stathopoulos, Bérengère Ize, Abdelrahim Zoued, Christian Cambillau, Christine Kellenberger, Alain Roussel, E. Cascales

### ► To cite this version:

Maxence S Vincent, Mickaël J Canestrari, Philippe Leone, Julien Stathopoulos, Bérengère Ize, et al.. Characterization of the *Porphyromonas gingivalis* Type IX Secretion Trans-envelope PorKLMNP Core Complex. *Journal of Biological Chemistry*, 2017, 292 (8), pp.3252 - 3261. 10.1074/jbc.M116.765081 . hal-01780705

**HAL Id: hal-01780705**

**<https://amu.hal.science/hal-01780705>**

Submitted on 27 Apr 2018

**HAL** is a multi-disciplinary open access archive for the deposit and dissemination of scientific research documents, whether they are published or not. The documents may come from teaching and research institutions in France or abroad, or from public or private research centers.

L'archive ouverte pluridisciplinaire **HAL**, est destinée au dépôt et à la diffusion de documents scientifiques de niveau recherche, publiés ou non, émanant des établissements d'enseignement et de recherche français ou étrangers, des laboratoires publics ou privés.

# Characterization of the *Porphyromonas gingivalis* Type IX Secretion Trans-Envelope PorKLMNP Core Complex\*

Maxence S. Vincent<sup>‡</sup>, Mickaël J. Canestrari<sup>‡</sup>, Philippe Leone<sup>¶,§</sup>, Julien Stathopoulos<sup>¶,§</sup>, Bérengère Ize<sup>‡</sup>, Abdelrahim Zoued<sup>‡</sup>, Christian Cambillau<sup>¶,§</sup>, Christine Kellenberger<sup>¶,§</sup>, Alain Roussel<sup>¶,§</sup>, and Eric Cascales<sup>‡,1</sup>

From <sup>‡</sup>Laboratoire d'Ingénierie des Systèmes Macromoléculaires, UMR7255, Institut de Microbiologie de la Méditerranée, Aix-Marseille Univ - CNRS, 31 Chemin Joseph Aiguier, 13402 Marseille Cedex 20, France; <sup>¶</sup>Architecture et Fonction des Macromolécules Biologiques, Centre National de la Recherche Scientifique, UMR 7257, Campus de Luminy, Case 932, 13288 Marseille Cedex 09, France and <sup>§</sup>Architecture et Fonction des Macromolécules Biologiques, Aix-Marseille Université, UMR 7257, Campus de Luminy, Case 932, 13288 Marseille Cedex 09, France.

**Running title:** T9SS membrane complex assembly

<sup>1</sup>To whom correspondence should be addressed. Laboratoire d'Ingénierie des Systèmes Macromoléculaires, UMR7255, Institut de Microbiologie de la Méditerranée, Aix-Marseille Univ - CNRS, 31 Chemin Joseph Aiguier, 13402 Marseille Cedex 20, France; Tel: +33 491-164-504; Fax: +33 491 712 124; E-mail: cascales@imm.cnrs.fr

\* This work was supported by the Centre National de la Recherche Scientifique (CNRS), the Aix-Marseille Université and a grant from the Agence Nationale de la Recherche (ANR-15-CE11-0019-01). MSV is a recipient of a doctoral fellowship from the French Ministère de la Recherche. The work of AZ was funded by a end-of-thesis fellowship from the Fondation pour la Recherche Médicale (FDT20140931060).

**Keywords:** Type IX secretion, T9SS, *Porphyromonas*, *Flavobacterium*, protein transport, gingipains, membrane complex, membrane proteins, gliding motility, gingivitis, periodontitis; protein secretion, toxins, channel.

---

## ABSTRACT

**The transport of proteins at the cell surface of *Bacteroidetes* depends on a secretory apparatus known as Type IX secretion system (T9SS). This machine is responsible for the cell surface exposition of various proteins such as adhesins required for gliding motility in *Flavobacteria*, S-layer components in *Tannerella forsythia* and tooth tissue-degrading enzymes in the oral pathogen *Porphyromonas gingivalis*. While a number of subunits of the T9SS have been identified, we lack details on the architecture of this secretion apparatus. Here we provide evidence that five of the genes encoding the core complex of the T9SS are co-transcribed, and that the gene products are distributed in the cell envelope. Protein-protein interaction studies then revealed that these proteins oligomerize and interact through a dense network of contacts.**

*Porphyromonas gingivalis* is the causative agent of gingivitis and periodontal diseases that are responsible for teeth loss (1, 2). It causes severe lesions in periodontal tissues such as the gingiva or the alveolar bone and yields to the disruption of the tooth-supporting structure (3). Periodontitis are considered a major public health concern as it affects ~ 35 % of the population. Tissue alterations and damages are mainly induced by a cocktail of toxin proteins secreted by the bacterium, the gingipains (4). Gingipains act as adhesins or proteases that help the bacterium to adhere to periodontal tissues and to promote gingival tissue invasion by the degradation of matrix proteins, fibrinogen and collagen (5, 6). The secretion of these proteins is a two-step mechanism: gingipains carry a N-terminal signal peptide and are first addressed to the periplasm by the Sec pathway before being transported to the cell surface or to the cell exterior (7). However, the machinery responsible for the translocation of gingipains through the outer membrane remained unknown as genes encoding a potential Type II secretion system (T2SS), the major two-step

secretory pathway, are absent in the *P. gingivalis* genome (8, 9). Recently, a number of proteins responsible for the active release of these proteins at the bacterial cell surface, named Por, have been identified (10-15). Although there is little evidence that these proteins assemble a secretion machine, they were collectively grouped under the name *Porphyromonas* secretion system (PorSS) and more recently, Type IX secretion system (T9SS) (10, 16). In addition to the gingipains, this secretion apparatus transports the Hbp35 haem-binding protein, the peptidylarginine deiminase (PPAD), a toxin responsible for host protein citrullination and rheumatoid arthritis, and Maf5, a subunit of the extracellular Maf fimbriae (17-19). Interestingly, most of the T9SS proteins share homologies with proteins encoded within genomes of species belonging to the *Bacteroidetes* phylum, such as *Flavobacterium*, *Capnocytophaga*, *Cellulophaga* or *Tannerella* (8). In these strains, the T9SS is responsible for the secretion of adhesins, chitinases or S-layer components (15, 20, 21). Although it has been proposed that the T9SS is a rotative machinery (22, 23), the overall organization and architecture of this secretion system are not known. In *P. gingivalis*, at least 14 genes are necessary for the function of the T9SS, including 3 regulators and 11 machine components (10, 24, 25). It has been reported that at least four of these components, PorK, PorL, PorM and PorN, assemble a > 1.4 MDa complex that resists blue native-polyacrylamide gel electrophoresis (10). The genes encoding these four proteins are contiguous on the chromosome and located downstream the gene encoding the PorP protein. Here, we show that the five genes are co-transcribed and we define the localization of the corresponding proteins. We further determine the topology of the PorL and PorM inner membrane proteins and provide insights into the protein-protein interactions within this complex.

## Results

*The porP, porK, porL, porM and porN genes are co-transcribed*—While most of the *por* genes required for gingipains secretion are scattered on the *P. gingivalis* genome, the *porP* (PGN\_1677), *porK* (PGN\_1676), *porL* (PGN\_1675), *porM* (PGN\_1674) and *porN* (PGN\_1673) genes are contiguous on the chromosome (Fig. 1A) and are only separated by few bases (*porP-porK*, 56-bp; *porK-porL*, 40-bp; *porL-porM*, 3-bp; *porM-porN*, 8-bp) (Fig. S1). The genomic organization and the

limited intergenic spaces suggest that the expression of these genes might be coordinated. To test whether the *porPKLMN* gene locus is transcribed as a unique polycistronic mRNA, we performed reverse-transcriptase - polymerase chain reactions (RT-PCR) using oligonucleotides designed for the amplification of each gene junction (named PK, KL, LM and MN respectively; see Fig. 1A). RT-PCR experiments were performed on purified total RNA extracted from *P. gingivalis* cells (Fig. 1B, upper panel). As controls, RT-PCR reactions were performed on purified genome DNA (Fig. 1B, middle panel), as well as on the total RNA preparation but in absence of reverse transcriptase to test for DNA contamination (Fig. 1B, lower panel). As shown on Fig. 1B, RT-PCR products with expected sizes were obtained for each gene junction of the *porPKLMN* gene cluster from DNA or cDNA, but not from RNA, suggesting that these five genes are co-transcribed.

*The PorKLMNP proteins are distributed in the cell envelope*—Four of the five gene products of the *porPKLMN* operon, PorK, -L, -M and -N, have been shown to assemble a > 1.4-MDa complex that resists blue native-polyacrylamide gel electrophoresis (10). To gain information on the sub-cellular localization of these proteins, we first performed *in silico* analyses to identify signal peptides or trans-membrane segments.

The *P. gingivalis* PorK protein (gene accession: GI:188595220) bears a signal sequence with a typical lipobox motif (Fig. S2). This motif comprises the highly conserved cysteine residue at position +1 of the mature protein, which is anticipated to be acylated. The +2 residue of the PorK protein, which defines the final localization of the lipoprotein, is a glycine. These analyses suggest that the *P. gingivalis* PorK protein is an outer membrane lipoprotein. Indeed, the PorK protein shares homologies with the *F. johnsoniae* GldJ and GldK proteins, two components of the gliding machinery, which have been experimentally demonstrated to be outer membrane lipoproteins (26).

The PorN (accession: GI:188595217) and PorP (accession: GI:188595221) proteins bear typical signal sequences and are likely exported to the periplasm (Fig. S2). By contrast, the PorL (accession: GI:188595219) and PorM (accession: GI:188595218) proteins have predicted trans-membrane helices (Fig. S3). To better define the localization of the PorL, PorM and PorP proteins,

we performed fractionation of *E. coli* cells expressing the corresponding genes fused to the FLAG epitope. Fig. 2A shows that PorL, PorM and PorP are associated with the membrane fraction. Dissociation of peripherally-associated membrane by sodium carbonate treatment of the total membrane fraction showed that these three subunits are integral membrane proteins (Fig. 2A). Finally, differential solubilization with sodium lauroyl sarcosinate (SLS), a detergent that specifically disrupts the inner membrane (Fig. 2B), and discontinuous sucrose gradient analyses (Fig. 2C and Fig. S4) demonstrated that PorP co-fractionates with outer membrane proteins whereas PorL - and putatively PorM - are inserted into the inner membrane. Although the results were less clear for PorM, cysteine accessibility assays (see below) confirmed that PorM is anchored to the inner membrane. PorP does not bear a lipobox motif, but rather is predicted to assemble a  $\beta$ -barrel structure. Indeed, Phyre analyses reported that PorP is likely to be an outer membrane barrel and a homology model could be built with 98% confidence using the structure of the *Ralstonia pickettii* toluene transporter TbuX protein (PDB: 3BRY) as template (Fig. 2D). Inner membrane proteins are usually embedded within the membrane via trans-membrane helices (TMH). Computer predictions and hydrophobicity plots of the PorL and PorM sequences suggested the existence of one or several TMH (Fig. S3). To test these predictions, we used a cysteine accessibility approach. This method is based on the accessibility of cysteine residues to 3-(*N*-maleimidyl-propionyl) biocytin (MPB), a sulfhydryl reagent that readily passes the OM but only inefficiently the IM of Gram-negative bacteria (27). Based on TMH predictions, cysteine substitutions were introduced into the cysteine-less PorL protein at various positions. MPB accessibility analyses in *E. coli* cells showed that only a cysteine positioned at residue 48 was labelled whereas cysteine residues located at position 17, 74, 275 and 302 remained inaccessible (Fig. 2E). These data demonstrate that PorL has cytoplasmic N- and C-termini and possesses two TMH located between residues 17-48 and 48-74 (Fig. 2E). The PorM protein possesses a native cysteine residue located at position 92 that is labelled by MPB. Cysteines were introduced into the PorM C92S variant, and MPB analyses showed that whereas a cysteine at position 9 was not accessible, cysteine residues at positions 41, 309 and 498 were labelled, demonstrating that PorM is a bitopic protein with in-to-out topology and a single membrane

spanning segment between residues 9 and 41 (Fig. 2F).

Based on these data we conclude that the PorK, -L, -M, -N and -P proteins are distributed into the cell envelope and comprises two inner membrane proteins (PorL and PorM), a periplasmic protein (PorN), and outer membrane lipoprotein (PorK) and  $\beta$ -barrel (PorP) (Fig. 2G).

#### *Bacterial two-hybrid and co-immunoprecipitation analyses define an intense interaction network—*

To gain insights on the architecture of the T9SS core complex, we next tested pair-wise interactions among the PorK, -L, -M, -N and -P proteins. First, interactions were assayed by bacterial two-hybrid. The T18 and T25 domains of the adenylate cyclase were fused to the N-termini of the PorL and PorM full-length subunits, and to the N- and C-termini of the soluble regions of PorK, -L, -M or -N proteins, as defined by topology experiments. The PorP  $\beta$ -barrel was not included in the assay. Fig. 3A shows that PorL and PorM oligomerize and interact with each other. The cytoplasmic segment of PorL comprised between the second trans-membrane segment and the C-terminal hydrophobic region (amino-acids 73-274) is sufficient to mediate oligomerization. By contrast, the PorL-PorM interaction does not involve the PorL cytoplasmic domain (PorL<sub>C</sub>), and therefore these data suggest that PorL and PorM interact through their trans-membrane segments. Fig. 3B reports the interactions between the PorM, PorK and PorN periplasmic fragments: the periplasmic soluble domain of PorM (PorM<sub>P</sub>), the soluble, unacylated, form of PorK and the PorN subunit. We showed that the periplasmic domain of PorM and the PorN protein oligomerize. In addition, this approach revealed an intense network of interaction in the periplasm: PorM<sub>P</sub> contacts PorK and PorN and the previously documented PorK-PorN interaction (28, 29).

The interactions between these four proteins, as well as PorP, were then tested by co-immune precipitations in the heterologous host *E. coli* (Fig. 3C). This approach confirmed the PorM-PorK, PorM-PorN and PorK-PorN interactions and revealed that PorP interacts with PorK and PorM (Fig. 3C). We did not detect interactions between PorL and PorK, PorL and PorN and PorN and PorP. The strength of the interaction between the PorM periplasmic domain and PorN was measured *in vitro* by bio-layer interferometry using the purified proteins (see below, Fig. 3D).

The two proteins interact with an apparent  $K_D$  of  $0.97 \pm 0.02 \mu\text{M}$ .

To gain further information on the oligomeric state of the Por subunits, the soluble fragments of PorK (unacylated form), PorL (cytoplasmic domain, PorL<sub>C</sub>, amino-acids 73-309), PorM (periplasmic domain, PorM<sub>P</sub>, amino-acids 36-516) and PorN (full-length mature protein) were fused to a N-terminal 6×His tag and subjected to purification using metal affinity chromatography and gel filtration. Although PorK remained insoluble, we succeeded to purify PorL<sub>C</sub>, PorM<sub>P</sub> and PorN (Fig. 4, A, B and C, left panels). The three proteins were subjected to size-exclusion chromatography (SEC) coupled to on-line multi-angle laser light scattering/quasi-elastic light scattering/absorbance/refractive index (MALS/QELS/UV/RI) analyses. Analyses of PorL<sub>C</sub> showed that this domain has a mass of 44 kDa (compared to the 29-kDa theoretical mass, Fig. 4A) suggesting that it has an elongated, non-compact conformation. PorL<sub>C</sub> elutes as two peaks (44 and 113 kDa) suggesting that it exists as monomer and trimer (Fig. 4A). Contrarily, PorM<sub>P</sub> (107 kDa compared to the 55-kDa theoretical mass, Fig. 4B) and PorN (94 kDa compared to the 43-kDa theoretical mass, Fig. 4C) exist both as dimers

## Discussion

In this study, we defined the localization and topology of the subunits of the *P. gingivalis* T9SS PorKLMNP complex. The five proteins are distributed in the cell envelope (Fig. 5): PorL and PorM are inner membrane proteins, PorN resides in the periplasm, whereas PorK and PorP are outer membrane lipoprotein and  $\beta$ -barrel, respectively. We then defined the interaction network between these subunits, demonstrating that PorL and PorM interact, likely through their transmembrane helices. PorM has a large periplasmic domain that mediates interaction with PorK, PorN and PorP. In addition to PorM, PorK contacts PorN and PorP (Fig 5). Recent studies showed that PorK and PorN interact with a 1:1 stoichiometry and assemble a ring-like structure composed of 32-36 PorKN heterodimers (28, 29). Taken together, these data provide evidence that PorKLMNP assemble a cell-envelope spanning complex, with a central protein, PorM, linking inner membrane (PorLM) and outer membrane-associated (PorKN) complexes. This situation is comparable to that of GspC, VirB10, TssM and TolA that connect IM and OM complexes in

T2SS, T4SS, T6SS and Tol-Pal systems, respectively (30-33).

The PorK, -L, -M and -N proteins were previously shown to assemble a stable > 1.4 MDa complex. Our results show that the *porP* gene is co-transcribed with the *porKLMN* genes and that PorP interacts with at least two components of this complex, PorM and PorK. However, Sato et al. reported that PorP is not part of and does not stabilize the > 1.4 MDa complex (10), suggesting that the interaction of PorP with the PorKLMN complex is more labile, prone to dissociation, or that PorP associates to the PorKLMN complex in specific conditions. Indeed, it has been shown that, contrarily to PorK, -L, -M and -N, PorP (or its homologue in *F. johnsoniae*, SprF) is an accessory component of the secretion apparatus as it is not required for the transport of all the T9SS substrates (34). However, a recent cross-linking study demonstrated that the PorKN outer membrane-associated complex interacts with an OM protein, PG0189 (29).

We also showed that PorL forms trimers whereas PorM and PorN dimerize. Although the oligomeric status of PorK was not defined in our study, the recent observation that PorK and PorN interact with a 1:1 stoichiometry (29) suggests a minimal PorK<sub>2</sub>L<sub>3</sub>M<sub>2</sub>N<sub>2</sub> complex. This minimal complex should have a mass of ~ 400 kDa. These data therefore suggest that either additional T9SS subunits are present in the > 1.4 MDa complex or that this complex results of the multimerization of the minimal PorK<sub>2</sub>L<sub>3</sub>M<sub>2</sub>N<sub>2</sub> complex. These two hypotheses are likely as (i) most secretion apparatus form large channels to accommodate folded effectors (35), (ii) multimerization has been reported for the T6SS TssJLM membrane complex that comprises five copies of dimers of TssJLM hetero-trimers (32), and (iii) additional components have been recently identified to interact with the PorKN complex (29).

It has been previously demonstrated that the T9SS is a two-step mechanism: the T9SS substrates are first exported through the inner membrane via the Sec translocon before being transported to the cell surface by the T9SS (7). However, our results stress that two proteins, PorL and PorM, are anchored to the inner membrane. Based on the localization/topology of these proteins and the recent evidence that the T9SS is a rotary machine (22, 23), we propose that PorL and PorM serve as an energy transducer complex to convert chemical energy (proton-motive force or ATP) into mechanical energy and provide the energy for

T9SS assembly, dynamics or for substrate translocation through the outer membrane. Energy transducers have been evidenced, notably in the case of the T4SS, in which the VirB10 protein transduces the energy provided by the VirB11, VirB4 and VirD4 ATPases to the VirB7/VirB9 outer membrane complex (31). However, none of the T9SS subunits bear signature of NTPases. By contrast, T9SS-dependent gliding motility has been shown to be dependent on the proton-motive force in *F. johnsoniae* (36). Energy transducers using the proton-motive force, such as the MotAB, TolQRA, ExbBD-TonB or AglQR complexes (37, 38), usually possess negatively charged glutamate or aspartate residues within the hydrophobic TMH. Interestingly, sequence analysis of PorL and PorM TMH defined in our study reveals that the second TMH of PorL, as well as the PorM TMH, bear glutamate residues that are conserved in the *F. johnsoniae* GldL and GldM homologues (Fig. S5). It would be therefore interesting to determine whether PorLM constitutes a new molecular motor and how these proteins power T9SS assembly or dynamics or substrate translocation.

Taken together, the data described in this study provide a better understanding of the *P. gingivalis* T9SS PorKLMNP complex and open new perspectives on the role of this complex in powering Type IX secretion. These data also pave the way for the design of specific inhibitors to prevent assembly of the PorKLMNP complex and hence to lessen or abolish *P. gingivalis* virulence.

## Experimental Procedures

**Bacterial strains, growth conditions, chemicals and antibodies**—The strains used in this study are listed in S1 Table. *Porphyromonas gingivalis* ATCC33277/DSM20709 (obtained from the DSMZ collection, Germany) was used as source of DNA for cloning. *P. gingivalis* cells were grown anaerobically in Brain Heart Infusion medium supplemented with menadiol (0.5 µg/mL) and haemin (5 µg/mL). *Escherichia coli* K-12 DH5α, W3110, BTH101 and Rosetta(DE3)pLys were used for cloning procedures, co-immune precipitations, two-hybrid and protein purification respectively. Unless specified, *E. coli* strains were routinely grown in LB medium at 37°C with shaking. Expression of genes from pBAD and pTet was induced for 40-45 min with L-arabinose 0.02% and anhydrotetracyclin (AHT) 0.1 µg/mL respectively. Plasmids were maintained by the addition of ampicillin (100 µg/mL), kanamycin

(50 µg/mL) or chloramphenicol (40 µg/mL). Igepal CA-630, L-arabinose and *N*-ethylmaleimide (NEM) were purchased from Sigma-Aldrich, and 3-(*N*-maleimidyl-propionyl) biocytin and alkaline phosphatase-conjugated streptavidin were purchased from Pierce. The anti-TolA, anti-TolB, anti-TolR, anti-OmpA and anti-OmpF polyclonal antibodies are from our laboratory collection, while the anti-EFTu (clone mAb900, Hycult Biotech), anti-FLAG (clone M2, Sigma Aldrich) and anti-VSVG (clone P5D4, Sigma-Aldrich) monoclonal antibodies are commercially available.

**RNA purification and Reverse Transcription-PCR**— $10^{10}$  *P. gingivalis* cells were resuspended in 1 mL of TE buffer (Tris-HCl 10 mM pH8.0, EDTA 1 mM) supplemented with lysozyme (50 mg/mL). Total RNAs were isolated using the Total RNA isolation system kit (Promega) and treated with 10 units of DNase (RTS DNase kit, MoBio). The concentration and the purity of the samples were measured at  $A_{260}$  and by the  $A_{260}/A_{280}$  ratio respectively using the nanodrop technology (Shimadzu BioSpec-nano). cDNA were then generated using the RT-PCR SuperScript first-strand synthesis kit (Invitrogen) using 100 ng of total RNAs and random hexamers. Polymerase chain reactions (PCR) were performed using the Q5 DNA polymerase (New England Biolabs) using 10 ng of genomic DNA (DNA), 10 ng of total RNA (RNA) or cDNA from 10 ng of total RNA (cDNA) as starting material.

**Plasmid construction**—The plasmids used for this study are listed in S1 Table. *por* genes were amplified from *P. gingivalis* genomic DNA extracted using the DNA purification kit (Qiagen) from  $6 \times 10^9$  cells. PCR were performed with a Biometra thermocycler, using the Phusion DNA polymerase (Thermo scientific) and custom oligonucleotides synthesized by Sigma Aldrich (listed in S1 Table). Expression plasmids were constructed by restriction-free cloning (39), as previously described (40). Briefly, the gene of interest was amplified using oligonucleotides introducing extensions annealing to the target vector. The double-stranded product of the first PCR has then been used as oligonucleotides for a second PCR using the target vector (pASK-IBA4, pASK-IBA37(+), pBAD33, pBAD24 or pLIC03) as template. PCR products were then treated with *DpnI* to eliminate template plasmids and transformed into DH5α-competent cells. BACTH plasmids were constructed by restriction-ligation. PCR products bearing 5' *XbaI* and 3' *KpnI* sites

were digested by the corresponding restriction enzymes (New England Biolabs) and inserted into pUT18 (fusion at the N-terminus of the T18 domain, X-T18), pUT18C (fusion at the C-terminus of the T18 domain, T18-X), pKT25 (fusion at the C-terminus of the T25 domain, T25-X) and pKTN25 (fusion at the N-terminus of the T25 domain, X-T25) vectors (41) digested with the same enzymes. All constructs have been verified by restriction analyses and DNA sequencing (GATC).

*Fractionation*—Cell fractionation assays have been performed as published (40, 42, 43). Briefly,  $2 \times 10^9$  exponentially growing cells were resuspended in 0.5 mL of Tris-HCl 10 mM (pH 8.0), sucrose 30% and incubated for 10 min on ice. After addition of 100  $\mu$ g/mL of lysozyme and 1 mM EDTA and further incubation for 45 min on ice, 0.5 mL of Tris-HCl 10 mM (pH 8.0) supplemented with DNase (200  $\mu$ g/mL) and  $MgCl_2$  (4 mM) were added and cells were lysed by five cycles of freeze and thaw. Unbroken cells were removed by centrifugation, and soluble and membrane fractions were separated by ultracentrifugation for 40 min at  $100,000 \times g$ . Membranes were washed with 20 mM Tris-HCl pH8.0,  $MgCl_2$  2 mM, resuspended in 1 ml of Tris-HCl 20 mM (pH8.0) supplemented with  $Na_2CO_3$  1M and incubated on a wheel for 1 h. The mixture was then ultracentrifuged for 40 min at  $100,000 \times g$  to separate integral membrane and peripherally membrane-associated proteins. Soluble and membrane-associated fractions were precipitated with trichloroacetic acid (15%), and resuspended in loading buffer prior to analysis by SDS-PAGE and immunoblotting. EF-Tu, TolA/TolR, TolB and OmpF were used as cytoplasmic, inner membrane, periplasmic and outer membrane markers, respectively.

*Differential membrane solubilization*—Sodium lauroyl sarcosinate is an anionic detergent that selectively disrupts the inner membrane and solubilises inner membrane proteins (44). Membranes prepared from  $10^{10}$  cells using the fractionation protocol were resuspended in 1 mL of Tris-HCl 10 mM (pH 8.0), EDTA 1 mM supplemented with 1% of sodium *N*-lauroyl sarcosinate (SLS; Sigma Aldrich) and incubated on a wheel for 1 h at room temperature (43). Insoluble (outer membrane) and soluble (inner membrane) fractions were collected by ultracentrifugation at  $100,000 \times g$  for 40 min prior to analysis by SDS-PAGE and immunoblotting.

*Sucrose sedimentation gradients*—Inner and outer membranes were separated using discontinuous sedimentation sucrose gradients as previously described (40, 42, 43).  $4 \times 10^{11}$  cells were harvested, resuspended in 3 mL of Tris-HCl 10 mM pH7.4, Sucrose 30% and RNase 100  $\mu$ g/mL, lysed by French press treatment (3 passages at 900 psi), and total membranes were recovered by centrifugation at  $100,000 \times g$  for 40 min and resuspended in 0.5 mL of 25% sucrose containing a protease inhibitor cocktail (Complete EDTA-free, Roche). The membrane fraction was then loaded on the top of a discontinuous sucrose gradient composed of the superposition of 1.5 mL of 30, 35, 40, 45, 50, 55, and 60% sucrose solutions (from top to bottom). Gradients were centrifuged at  $90,000 \times g$  for 90 hours and 500  $\mu$ L fractions were collected from the top. The fractions were analysed by a NADH oxidase enzymatic test, and by SDS-PAGE and immunodetection. TolA and OmpF were used as inner and outer membrane markers, respectively. The NADH oxidase activity was measured in 96-well polystyrene microtitre dishes, using 20  $\mu$ L of each fraction diluted in 180  $\mu$ L of Tris-HCl 50 mM pH7.5, dithiothreitol (DTT) 0.2 mM and NADH 0.5 mM. The decrease of absorbance of the NADH at 340 nm, which reflects the activity of the NADH oxidase, was measured every min at 25°C using a TECAN M200 microplate reader, and the slope was calculated. Each fraction has been tested in triplicate. NADH oxidase activities are reported as the percentage of activity in the fraction compared to the total membrane fraction.

*Cysteine accessibility experiments (SCAM)*—Cysteine accessibility experiments (27) were carried out as described on whole cells (40, 43, 45, 46) with modifications. Briefly,  $2 \times 10^{10}$  cells producing the cysteine variant were harvested, resuspended in buffer A (Hepes 100 mM pH 7.5, sucrose 250 mM,  $MgCl_2$  25 mM, KCl 0.1 mM) to a final  $A_{600nm}$  of 12. 3-(*N*-maleimidyl-propionyl) biocytin (MPB; Molecular Probes) was added to a final concentration of 100  $\mu$ M (from a 20 mM stock freshly dissolved in DMSO) and the cells were incubated for 30 min at 25°C.  $\beta$ -Mercaptoethanol (20 mM final concentration) was added to quench the biotinylation reaction, and cells were washed and resuspended in buffer A supplemented with *N*-ethyl maleimide 5 mM to block all free sulfhydryl residues. After incubation 20 min at 25°C, cells were disrupted by sonication. Membranes recovered by ultracentrifugation 40 min at  $100,000 \times g$  were resuspended in 1 mL of buffer B (Tris-HCl 10

mM pH 8.0, NaCl 100 mM, Triton X-100 1% (v/v)) supplemented with protease inhibitor cocktail (Complete, Roche). After incubation on a wheel for 1 hour, insoluble material was discarded by centrifugation 15 min. at  $20,000 \times g$ , and solubilized proteins were subjected to immune precipitation using anti-FLAG-conjugated beads (M2 clone, Sigma Aldrich). After 3 hours of incubation on a wheel, beads were washed twice with 1 mL of buffer B, once with buffer B supplemented with Tween 0.1%, and once with buffer C (Tris-HCl 10 mM, pH 8.0, NaCl 100 mM, Triton X-100 0.1% (v/v)). Beads were air-dried, resuspended and boiled in Laemmli buffer prior to SDS-PAGE analysis and immuno-detection with anti-FLAG antibodies (to detect the proteins) or streptavidin (to detect the biotinylated proteins) coupled to alkaline phosphatase. Control experiments were performed on purified membranes instead of whole cells.

*Bacterial two-hybrid*—Protein-protein interactions were assessed with the adenylate cyclase-based two-hybrid technique (41) using previously published protocols (47). Briefly, the proteins to be tested were fused to the isolated T18 and T25 catalytic domains of the *Bordetella* adenylate cyclase. After introduction of the two plasmids producing the fusion proteins into the reporter BTH101 strain, plates were incubated at 30°C for 48 hours. Three independent colonies for each transformation were inoculated into 600  $\mu$ L of LB medium supplemented with ampicillin, kanamycin and IPTG (0.5 mM). After overnight growth at 30°C, 10  $\mu$ L of each culture were dropped onto LB plates supplemented with ampicillin, kanamycin, IPTG and X-Gal and incubated for 16 hours at 30 °C. Controls include interaction assays with TolB/Pal, or MalF/MalG, two protein pairs unrelated to the T9SS. The experiments were done at least in triplicate and a representative result is shown.

*Co-immune precipitation*— $10^{11}$  exponentially growing cells were harvested, resuspended in 50 mM Tris-HCl pH7.2, 0.5 M NaCl and 12% PEG3350 supplemented with lysozyme (100  $\mu$ g/mL) and DNase (100  $\mu$ g/mL) and broken by three passages at the French press (900 psi). Unbroken cells were discarded and lysates corresponding to  $10^{10}$  cells were mixed. The mixture was sonicated (6 pulses, 80% duty; Branson sonifier), incubated for 15 min. at 37°C and sonicated (4 pulses, 80% duty) before being diluted in three volumes of 20 mM Tris-HCl pH7.2, EDTA 1.35 mM, Igepal CA-630 0.2% supplemented with protease inhibitors (Complete,

Roche). After 1 hour of incubation on a wheel, insoluble material was discarded by centrifugation 15 min. at  $20,000 \times g$ , and solubilized proteins were subjected to immune precipitation using anti-FLAG-conjugated agarose beads (clone M2, Sigma Aldrich) for 16 hours on a wheel at 4°C. The beads were washed twice with 1 mL of 20 mM Tris-HCl pH7.2, NaCl 125 mM, EDTA, 1 mM, 3% PEG3350 and Igepal CA-630 0.1% and once with the same buffer without detergent. Beads were air-dried, resuspended and boiled in Laemmli buffer prior to SDS-PAGE analysis and immuno-detection with anti-FLAG and anti-VSVG monoclonal antibodies coupled to alkaline phosphatase.

*Protein purification*—Proteins were purified from Rosetta(DE3) pLysS *E. coli* cells (Novagen) producing the PorN protein or the Por<sub>L</sub>C or Por<sub>M</sub>P fragments cloned into the pLIC03 vector (kindly provided by the BioXtal company; unpublished). The pLIC03 vector has been designed for ligation-independent cloning (LIC; (48)) and is a derivative of the pET28a+ expression vector (Novagen) in which a cassette coding for a 6 $\times$ His-tag and a Tobacco Etch Virus (TEV) protease cleavage site followed by the suicide gene *sacB* flanked by *Bsa*I restriction sites was introduced downstream the ATG start codon. Cells were grown in ZYP-5052 auto-induction media (49) at 37°C for 4 hours followed by 18-hour growth at 17°C. Cells were harvested by centrifugation ( $4000 \times g$  for 10 min) and the pellet was homogenized and frozen in lysis buffer (50 mM Tris-HCl pH8.0, 300 mM NaCl, 10 mM imidazole, 0.1 mg/mL lysozyme, 1 mM phenylmethylsulfonyl fluoride (PMSF)). After thawing, DNase I (20  $\mu$ g/mL) and MgSO<sub>4</sub> (1 mM) were added and cells were lysed by sonication. The pellet and soluble fractions were separated by centrifugation ( $16,000 \times g$  for 30 min) and the proteins were purified from the soluble fraction by immobilized metal ion affinity chromatography using a 5 mL HisTrap crude (GE Healthcare) Ni<sup>2+</sup>-chelating column equilibrated in buffer A (50 mM Tris-HCl pH8.0, 300 mM NaCl, 10 mM imidazole). The proteins were eluted with buffer A supplemented with 250 mM imidazole and was further purified by a size exclusion chromatography (HiLoad 16/60 Superdex 200 prep grade, GE) equilibrated in 10 mM Hepes pH7.5, 150 mM NaCl. For the biophysical assays, the proteins were concentrated by centrifugation using 10- or 30-kDa cut-off Amicon concentrators, in the same buffer as for exclusion chromatography, to 5 mg/mL. The protein

concentration was determined by the absorbance of the sample at 280 nm using a NanoDrop 2000 (Thermo Scientific).

**Biophysical assays**—The biophysical methods were performed as previously published (50, 51). **Multi Angle Light Scattering analysis (MALS)**. Size exclusion chromatography was carried out on an Alliance 2695 HPLC system (Waters) using a Silica Gel KW803 column (Shodex) equilibrated in 10 mM Hepes pH 7.5, 150 mM NaCl at a flow of 0.5 mL/min. Detection was performed using a triple-angle light scattering detector (Mini-DAWN TREOS, Wyatt Technology), a quasi-elastic light scattering instrument (Dynapro, Wyatt Technology), and a differential refractometer (OptilabrEX, Wyatt Technology). **Bio-layer interferometry (BLI)**. The purified PorN protein was first biotinylated using the EZ-Link NHS-PEG4-Biotin kit (Perbio Science, France). The reaction was quenched by removing the excess of biotin using a Zeba Spin Desalting column (Perbio Science, France). BLI studies were performed in black 96-well plates (Greiner) at 25°C using an OctetRed96 (ForteBio, USA). Streptavidin biosensor tips (ForteBio, USA) were first hydrated with 0.2 mL Kinetic buffer (KB, ForteBio, USA) for 20 min and then loaded with biotinylated PorN (10 µg/mL in KB). The association of PorN with various concentrations of PorM<sub>P</sub> (0.27 µM, 0.83 µM, 2.5 µM, 7.6 µM and 23 µM) was monitored for 600 sec, and the dissociation was followed for 1,800 sec. in KB. Fitting of the data and constants measurements (statistical parameters: Chi<sup>2</sup>=2.76; R<sup>2</sup>=0.99) were performed with the Octet Red system software (version 7.1) using the 1:1 model. Independent experiments were run to verify that no nonspecific binding occurred, using biosensors loaded with a fragment antigen-binding (Fab) or with no protein.

**Computer analyses and structure modeling**—Sequence signal and lipoprotein motifs were predicted using PSORTb (52), SignalP (53) and LipoP (54). Trans-membrane helix predictions were made using HMMTop (55), TMHMM (56), TMpred (57) and PHDhtm (58). Secondary structure predictions were made using the Pspred server (<http://bioinf.cs.ucl.ac.uk/psipred/>). Structural predictions and homology modelling of the tri-dimensional structure of PorP were performed using HHpred (59) and Swiss-Model (60) using the 3.2-Å X-ray structure of the *Ralstonia pickettii* toluene transporter TbuX protein (PDB: 3BRY) (confidence= 98%).

**Miscellaneous**—SDS-polyacrylamide gel electrophoresis was performed using standard protocols. For immunostaining, proteins were transferred onto nitrocellulose membranes and immunoblots were probed with primary antibodies and goat secondary antibodies coupled to alkaline phosphatase, and developed in alkaline buffer in presence of 5-bromo-4-chloro-3-indolylphosphate and nitroblue tetrazolium.

**Author contributions**—M.S.V., M.J.C., B.I. and A.Z. performed the *in vivo* experiments. P.L., J.S. and C.K. purified the proteins and performed the *in vitro* experiments. C.C., A.R. and E.C. conceived and coordinated the study. M.S.V, P.L., A.R. and E.C. designed the experiments and prepared figures. E.C. wrote the paper. All authors analyzed the results and approved the final version of the manuscript.

**Conflict of interest**—The authors declare that they have no conflicts of interest with the contents of this article.

**Acknowledgements**—We thank Laure Journet and Eric Durand for critical reading of the manuscript, Romain Borne, Pascale de Philip and Henri-Pierre Fiérobe for advices regarding growth of *P. gingivalis*, Haensel Fletcher and Margaret Duncan for providing protocols, Antoine Schramm and Jean-Pierre Duneau for insights regarding the PorP homology model, the members of the Cascales, Cambillau/Roussel, Llobès, Sturgis and Bouveret research groups for discussion, Isabelle Bringer, Annick Brun and Olivier Uderso for technical assistance and Kelly Diote for encouragements.

## References

1. Nakayama, K. (2015) *Porphyromonas gingivalis* and related bacteria: from colonial pigmentation to the type IX secretion system and gliding motility. *J Periodontol Res.* **50**,1-8.
2. Sakamoto, M., Umeda, M., and Benno, Y. (2005) Molecular analysis of human oral microbiota. *J Periodont Res.* **40**, 277–285.
3. Rôças, I.N., Siqueira, J.F. Jr, Santos, K.R., and Coelho, A.M. (2001) "Red complex" (*Bacteroides forsythus*, *Porphyromonas gingivalis*, and *Treponema denticola*) in endodontic infections: a molecular approach.

- Oral Surg Oral Med Oral Pathol Oral Radiol Endod.* **91**, 468-471.
4. Potempa, J., Sroka, A., Imamura, T., and Travis, J. (2003) Gingipains, the major cysteine proteinases and virulence factors of *Porphyromonas gingivalis*: structure, function and assembly of multidomain protein complexes. *Curr Protein Pept Sci.* **4**, 397-407.
  5. Boisvert, H., Lorand, L., and Duncan, M.J. (2014) Transglutaminase 2 is essential for adherence of *Porphyromonas gingivalis* to host cells. *Proc Natl Acad Sci USA.* **111**, 5355-5360.
  6. Boisvert, H., and Duncan, M.J. (2010) Translocation of *Porphyromonas gingivalis* gingipain adhesin peptide A44 to host mitochondria prevents apoptosis. *Infect Immun.* **78**, 3616-3624.
  7. Veith, P.D., Nor Muhammad, N.A., Dashper, S.G., Likić, V.A., Gorasia, D.G., Chen, D., Byrne, S.J., Catmull, D.V., and Reynolds, E.C. (2013) Protein substrates of a novel secretion system are numerous in the Bacteroidetes phylum and have in common a cleavable C-terminal secretion signal, extensive post-translational modification, and cell-surface attachment. *J Proteome Res.* **12**, 4449-4461.
  8. McBride, M.J., and Zhu, Y. (2013) Gliding motility and Por secretion system genes are widespread among members of the phylum bacteroidetes. *J Bacteriol.* **195**, 270-278.
  9. Abby, S.S., Cury, J., Guglielmini, J., Néron, B., Touchon, M., and Rocha, E.P. (2016) Identification of protein secretion systems in bacterial genomes. *Sci Rep.* **6**, 23080.
  10. Sato, K., Naito, M., Yukitake, H., Hirakawa, H., Shoji, M., McBride, M.J., Rhodes, R.G., and Nakayama, K. (2010) A protein secretion system linked to bacteroidete gliding motility and pathogenesis. *Proc Natl Acad Sci USA.* **107**, 276-281.
  11. Glew, M.D., Veith, P.D., Peng, B., Chen, Y.Y., Gorasia, D.G., Yang, Q., Slakeski, N., Chen, D., Moore, C., Crawford, S., and Reynolds, E.C. (2012) PG0026 is the C-terminal signal peptidase of a novel secretion system of *Porphyromonas gingivalis*. *J Biol Chem.* **287**, 24605-24617.
  12. Chen, Y.Y., Peng, B., Yang, Q., Glew, M.D., Veith, P.D., Cross, K.J., Goldie, K.N., Chen, D., O'Brien-Simpson, N., Dashper, S.G., and Reynolds, E.C. (2011) The outer membrane protein LptO is essential for the O-deacylation of LPS and the co-ordinated secretion and attachment of A-LPS and CTD proteins in *Porphyromonas gingivalis*. *Mol Microbiol.* **79**, 1380-1401.
  13. Kharade, S.S., and McBride, M.J. (2015) *Flavobacterium johnsoniae* PorV is required for secretion of a subset of proteins targeted to the type IX secretion system. *J Bacteriol.* **197**, 147-158.
  14. Taguchi, Y., Sato, K., Yukitake, H., Inoue, T., Nakayama, M., Naito, M., Kondo, Y., Kano, K., Hoshino, T., Nakayama, K., Takashiba, S., and Ohara, N. (2015) Involvement of an Skp-like protein, PGN\_0300, in the Type IX secretion system of *Porphyromonas gingivalis*. *Infect Immun.* **84**, 230-240.
  15. Shrivastava, A., Johnston, J.J., van Baaren, J.M., and McBride, M.J. (2013) *Flavobacterium johnsoniae* GldK, GldL, GldM, and SprA are required for secretion of the cell surface gliding motility adhesins SprB and RemA. *J Bacteriol.* **195**, 3201-3212.
  16. Sato, K., Yukitake, H., Narita, Y., Shoji, M., Naito, M., and Nakayama, K. (2013) Identification of *Porphyromonas gingivalis* proteins secreted by the Por secretion system. *FEMS Microbiol Lett.* **338**, 68-76.
  17. Shoji, M., Sato, K., Yukitake, H., Kondo, Y., Narita, Y., Kadowaki, T., Naito, M., and Nakayama, K. (2011) Por secretion system-dependent secretion and glycosylation of *Porphyromonas gingivalis* hemin binding protein 35. *PLoS One.* **6**, e21372.
  18. Goulas, T., Mizgalska, D., Garcia-Ferrer, I., Kantyka, T., Guevara, T., Szmigielski, B., Sroka, A., Millán, C., Usón, I., Veillard, F., Potempa, B., Mydel, P., Solà, M., Potempa, J., and Gomis-Rüth, F.X. (2015) Structure and mechanism of a bacterial host protein citrullinating virulence factor, *Porphyromonas gingivalis* peptidylarginine deiminase. *Sci Rep.* **5**, 11969.
  19. Hasegawa, Y., Iijima, Y., Persson, K., Nagano, K., Yoshida, Y., Lamont, R.J., Kikuchi, T., Mitani, A., and Yoshimura, F. (2016) Role of Mfa5 in expression of Mfa1 fimbriae in *Porphyromonas gingivalis*. *J Dent Res.* **95**, 1291-1297.
  20. Narita, Y., Sato, K., Yukitake, H., Shoji, M., Nakane, D., Nagano, K., Yoshimura, F., Naito, M., and Nakayama, K. (2014) Lack of a surface layer in *Tannerella forsythia* mutants deficient in the type IX secretion system. *Microbiology.* **160**, 2295-2303.

21. Tomek, M.B., Neumann, L., Nimeth, I., Koerdts, A., Andesner, P., Messner, P., Mach, L., Potempa, J.S., and Schäffer, C. (2014) The S-layer proteins of *Tannerella forsythia* are secreted via a type IX secretion system that is decoupled from protein O-glycosylation. *Mol Oral Microbiol.* **29**, 307-320.
22. Shrivastava, A., Lele, P.P., and Berg, H.C. (2015) A rotary motor drives *Flavobacterium* gliding. *Curr Biol.* **25**, 338-341.
23. Shrivastava, A., and Berg, H.C. (2015) Towards a model for *Flavobacterium* gliding. *Curr Opin Microbiol.* **28**, 93-97.
24. Kadowaki, T., Yukitake, H., Naito, M., Sato, K., Kikuchi, Y., Kondo, Y., Shoji, M., and Nakayama, K. (2016) A two-component system regulates gene expression of the type IX secretion component proteins via an ECF sigma factor. *Sci Rep.* **6**, 23288.
25. Vincent, M.S., Durand, E., and Cascales, E. (2016) The PorX response regulator of the *Porphyromonas gingivalis* PorXY two-component system does not directly regulate the Type IX secretion genes but binds the PorL subunit. *Front Cell Infect Microbiol.* **6**, 96.
26. Braun, T.F., and McBride, M.J. (2005) *Flavobacterium johnsoniae* GldJ is a lipoprotein that is required for gliding motility. *J Bacteriol.* **187**, 2628-2637.
27. Bogdanov, M., Zhang, W., Xie, J., and Dowhan, W. (2005) Transmembrane protein topology mapping by the substituted cysteine accessibility method (SCAM(TM)): application to lipid-specific membrane protein topogenesis. *Methods.* **36**, 148-171.
28. Glew, M.D., Veith, P.D., Chen, D., Seers, C.A., Chen, Y.Y., and Reynolds, E.C. (2014) Blue native-PAGE analysis of membrane protein complexes in *Porphyromonas gingivalis*. *J Proteomics.* **110**, 72-92.
29. Gorasia, D.G., Veith, P.D., Hanssen, E.G., Glew, M.D., Sato, K., Yukitake, H., Nakayama, K., and Reynolds, E.C. (2016) Structural insights into the PorK and PorN components of the *Porphyromonas gingivalis* Type IX secretion system. *PLoS Pathog.* **12**:e1005820.
30. Korotkov, K.V., Johnson, T.L., Jobling, M.G., Pruneda, J., Pardon, E., Héroux, A., Turley, S., Steyaert, J., Holmes, R.K., Sandkvist, M., and Hol, W.G. (2011) Structural and functional studies on the interaction of GspC and GspD in the type II secretion system. *PLoS Pathog.* **7**, e1002228.
31. Cascales, E., and Christie, P.J. (2004) *Agrobacterium* VirB10, an ATP energy sensor required for type IV secretion. *Proc Natl Acad Sci USA.* **101**, 17228-17233.
32. Durand, E., Nguyen, V.S., Zoued, A., Logger, L., Péhau-Arnaudet, G., Aschtgen, M.S., Spinelli, S., Desmyter, A., Bardiaux, B., Dujancourt, A., Roussel, A., Cambillau, C., Cascales, E., and Fronzes, R. (2015) Biogenesis and structure of a type VI secretion membrane core complex. *Nature.* **523**, 555-560.
33. Llobès, R., Cascales, E., Walburger, A., Bouveret, E., Lazdunski, C., Bernadac, A., and Journet, L. (2001) The Tol-Pal proteins of the *Escherichia coli* cell envelope: an energized system required for outer membrane integrity? *Res Microbiol.* **152**, 523-529.
34. Rhodes, R.G., Nelson, S.S., Pochiraju, S., and McBride, M.J. (2011) *Flavobacterium johnsoniae* *sprB* is part of an operon spanning the additional gliding motility genes *sprC*, *sprD*, and *sprF*. *J Bacteriol.* **193**, 599-610.
35. Costa, T.R., Felisberto-Rodrigues, C., Meir, A., Prevost, M.S., Redzej, A., Trokter, M., and Waksman, G. (2015) Secretion systems in Gram-negative bacteria: structural and mechanistic insights. *Nat Rev Microbiol.* **13**, 343-359.
36. Nakane, D., Sato, K., Wada, H., McBride, M.J., and Nakayama, K. (2013) Helical flow of surface protein required for bacterial gliding motility. *Proc Natl Acad Sci USA.* **110**, 11145-11150.
37. Cascales, E., Llobès, R., and Sturgis, J.N. (2001) The TolQ-TolR proteins energize TolA and share homologies with the flagellar motor proteins MotA-MotB. *Mol Microbiol.* **42**, 795-807.
38. Sun, M., Wartel, M., Cascales, E., Shaevitz, J.W., and Mignot, T. (2011) Motor-driven intracellular transport powers bacterial gliding motility. *Proc Natl Acad Sci USA.* **108**, 7559-7564.
39. van den Ent, F., and Löwe, J. (2006) RF cloning: a restriction-free method for inserting target genes into plasmids. *J Biochem Biophys Methods.* **67**, 67-74.
40. Aschtgen, M.S., Gavioli, M., Dessen, A., Llobès, R., and Cascales, E. (2010) The SciZ protein anchors the enteroaggregative *Escherichia coli* Type VI secretion system to the cell wall. *Mol Microbiol.* **75**, 886-899.

41. Karimova, G., Pidoux, J., Ullmann, A., and Ladant, D. (1998) A bacterial two-hybrid system based on a reconstituted signal transduction pathway. *Proc Natl Acad Sci USA*. **95**, 5752-5756.
42. Aschtgen, M.S., Bernard, C.S., de Bentzmann, S., Llobès, R., and Cascales, E. (2008) SciN is an outer membrane lipoprotein required for type VI secretion in enteroaggregative *Escherichia coli*. *J Bacteriol*. **190**, 7523-7531.
43. Aschtgen, M.S., Zoued, A., Llobès, R., Journet, L., and Cascales, E. (2012) The C-tail anchored TssL subunit, an essential protein of the enteroaggregative *Escherichia coli* Sci-1 Type VI secretion system, is inserted by YidC. *Microbiologyopen*. **1**, 71-82.
44. Filip, C., Fletcher, G., Wulff, J.L., and Earhart, C.F. (1973) Solubilization of the cytoplasmic membrane of *Escherichia coli* by the ionic detergent sodium-lauryl sarcosinate. *J Bacteriol*. **115**, 717-722.
45. Jakubowski, S.J., Krishnamoorthy, V., Cascales, E., and Christie, P.J. (2004) *Agrobacterium tumefaciens* VirB6 domains direct the ordered export of a DNA substrate through a type IV secretion System. *J Mol Biol*. **341**, 961-977.
46. Goemaere, E.L., Devert, A., Llobès, R., and Cascales, E. (2007) Movements of the TolR C-terminal domain depend on TolQR ionizable key residues and regulate activity of the Tol complex. *J Biol Chem*. **282**, 17749-17757.
47. Zoued, A., Durand, E., Brunet, Y.R., Spinelli, S., Douzi, B., Guzzo, M., Flaugnatti, N., Legrand, P., Journet, L., Fronzes, R., Mignot, T., Cambillau, C., and Cascales, E. (2016) Priming and polymerization of a bacterial contractile tail structure. *Nature*. **531**, 59-63.
48. Aslanidis, C., and de Jong, P.J. (1990) Ligation-independent cloning of PCR products (LIC-PCR). *Nucleic Acids Res*. **18**, 6069-6074.
49. Studier, F.W. (2005) Protein production by auto-induction in high-density shaking cultures. *Prot. Exp. Pur*. **41**, 207-234.
50. Felisberto-Rodrigues, C., Durand, E., Aschtgen, M.S., Blangy, S., Ortiz-Lombardia, M., Douzi, B., Cambillau, C., and Cascales, E. (2011) Towards a structural comprehension of bacterial type VI secretion systems: characterization of the TssJ-TssM complex of an *Escherichia coli* pathovar. *PLoS Pathog*. **7**, e1002386.
51. Flaugnatti, N., Le, T.T., Canaan, S., Aschtgen, M.S., Nguyen, V.S., Blangy, S., Kellenberger, C., Roussel, A., Cambillau, C., Cascales, E., and Journet, L. (2016) A phospholipase A1 antibacterial Type VI secretion effector interacts directly with the C-terminal domain of the VgrG spike protein for delivery. *Mol Microbiol*. **99**, 1099-1118.
52. Yu, N.Y., Wagner, J.R., Laird, M.R., Melli, G., Rey, S., Lo, R., Dao, P., Sahinalp, S.C., Ester, M., Foster, L.J., and Brinkman, F.S. (2010) PSORTb 3.0: improved protein subcellular localization prediction with refined localization subcategories and predictive capabilities for all prokaryotes. *Bioinformatics*. **26**, 1608-1615.
53. Petersen, T.N., Brunak, S., von Heijne, G., and Nielsen, H. (2011) SignalP 4.0: discriminating signal peptides from transmembrane regions. *Nat Methods*. **8**, 785-786.
54. Juncker, A.S., Willenbrock, H., von Heijne, G., Brunak, S., Nielsen, H., and Krogh, A. (2003) Prediction of lipoprotein signal peptides in Gram-negative bacteria. *Protein Sci*. **12**, 1652-1662.
55. Tusnády, G.E., and Simon, I. (1998) Principles governing amino acid composition of integral membrane proteins: application to topology prediction. *J Mol Biol*. **283**, 489-506.
56. Krogh, A., Larsson, B., von Heijne, G., and Sonnhammer, E.L. (2001) Predicting transmembrane protein topology with a hidden Markov model: application to complete genomes. *J Mol Biol*. **305**, 567-580.
57. Hofmann, K., and Stoffel, W. (1993) A database of membrane spanning protein segments. *Biol. Chem*. **374**, 166.
58. Rost, B., Fariselli, P., and Casadio, R. (1996) Topology prediction for helical transmembrane proteins at 86% accuracy. *Protein Sci*. **5**, 1704-1718.
59. Söding, J., Biegert, A., and Lupas, A.N. (2005) The HHpred interactive server for protein homology detection and structure prediction. *Nucleic Acids Res*. **33**, W244-8.
60. Biasini, M., Bienert, S., Waterhouse, A., Arnold, K., Studer, G., Schmidt, T., Kiefer, F., Gallo Cassarino, T., Bertoni, M., Bordoli, L., and Schwede, T. (2014) SWISS-MODEL: modelling protein tertiary and quaternary structure using evolutionary information. *Nucleic Acids Res*. **42**, W252-8.

## LEGEND TO FIGURES

FIGURE 1. **The *porP*, *porK*, *porL*, *porM* and *porN* genes are co-transcribed.** *A*, Schematic organization of the *Porphyromonas gingivalis* *porP-K-L-M-N* fragment (PGN\_1677 to PGN\_1673). The fragments corresponding to gene junctions and amplified in the RT-PCR experiments are indicated below (PK, 393-bp; KL, 377-bp; LM, 423-bp; MN, 432-bp). *B*, Operon structure of the *P. gingivalis* *porP-K-L-M-N* fragment. Agarose gel analyses of the indicated gene junctions amplified by PCR from cDNA (upper panel), genomic DNA (middle panel; positive control) and total RNA (lower panel, negative control). The presence of PCR fragment in the cDNA gels demonstrates co-transcription of the genes located in 5' and 3' of the amplified region. Molecular weight markers (MW, in kb) are indicated on the left.

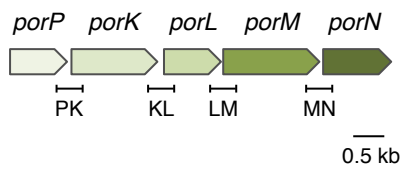
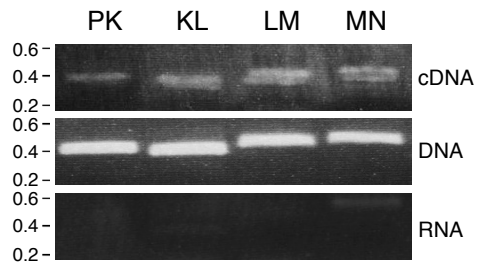
FIGURE 2. **Localization and topologies of the PorL, PorM, PorN and PorP proteins.** *A*, PorL, PorM and PorP co-fractionate with integral membrane proteins. *E. coli* cells producing FLAG-tagged PorL, PorM or PorP (T, Total fraction) were fractionated to separate soluble (S), and membrane (M) fractions. Membranes were then treated with sodium carbonate (Na<sub>2</sub>CO<sub>3</sub>) to separate peripheral membrane (P) and integral membrane (I) proteins. Samples from 5×10<sup>8</sup> cells were subjected to 12.5%-acrylamide SDS-PAGE and immunodetected with antibodies directed against the EFTu (soluble), TolB (soluble and peripherally associated to membrane) and TolA (integral inner membrane) proteins, and the FLAG epitope. *B*, Total membranes from *E. coli* cells producing FLAG-tagged PorP, PorL or PorM were subjected to solubilization with Sodium Lauroyl Sarcosinate (SLS). Solubilized inner membrane (IM) and insolubilized outer membrane (OM) proteins were separated. Samples from 5×10<sup>8</sup> cells were subjected to 12.5%-acrylamide SDS-PAGE and immunodetected with antibodies directed against the TolR (inner membrane), OmpA (outer membrane) proteins, and the FLAG epitope. *C*, Total membranes from *E. coli* cells producing FLAG-tagged PorL, PorM or PorP were separated on a discontinuous sedimentation sucrose gradient. The collected fractions were analyzed for contents using anti-FLAG antibodies. The positions of the inner (plain lines) and outer membrane (dotted lines) fractions, based on immunodetection controls with anti-TolA (inner membrane) and anti-OmpF/anti-Pal (outer membrane) antibodies and with a NADH oxidase (inner membrane) activity test (Fig. S4), are indicated. Molecular weight markers are indicated on the left of each panel. *D*, Homology model of the PorP protein based on the crystal structure of the *Ralstonia pickettii* toluene transporter TbuX protein (PDB: 3BRY) generated using HHPred/Swiss-Model. *E* and *F*, Accessibility of cysteine residues. Whole cells (upper panel) or total membrane (middle panel) of *E. coli* cells producing the FLAG-tagged PorL (*E*) or PorM (*F*) wild-type (WT) or cysteine-substituted derivatives were treated with the 3-(*N*-maleimidyl-propionyl) biocytin (MPB) probe, solubilized, and the PorL and PorM proteins were immuno-precipitated using agarose beads coupled to M2 anti-FLAG antibody. Precipitated material was subjected to SDS-PAGE and Western blot analysis using anti-FLAG antibody (to detect PorL or PorM, lower panel) and streptavidin coupled to alkaline phosphatase (to detect biotinylated PorL or PorM derivatives). Molecular weight markers are indicated on the left. *G*, Topology model for the PorL and PorM proteins at the inner membrane based on the cysteine-accessibility experiments. The positions of the labelled and unlabelled cysteine residues are indicated by open and filled circles, respectively.

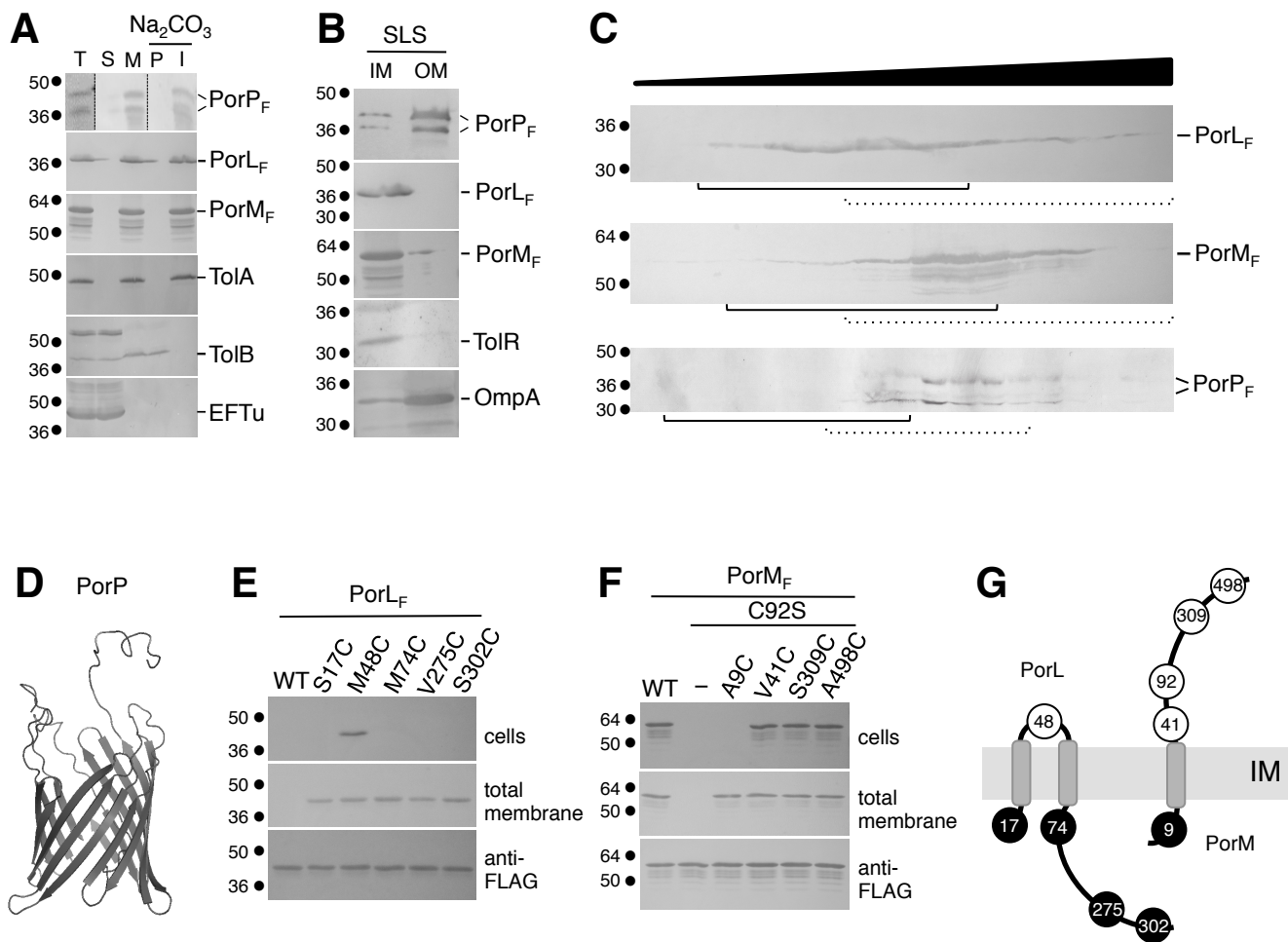
FIGURE 3. **Interaction network among the PorKLMNP complex.** *A* and *B*, Bacterial two-hybrid assay. BTH101 reporter cells producing the indicated proteins or domains (PorL<sub>C</sub>, cytoplasmic domain of the PorL protein; PorL<sub>CΔC6</sub>, cytoplasmic domain of the PorL protein deleted of the C-terminal hydrophobic helix) fused to the T18 or T25 domain of the *Bordetella* adenylate cyclase were spotted on plates supplemented with IPTG and the chromogenic substrate X-Gal. Interaction between the two fusion proteins is attested by the dark blue color of the colony. The MalF-MalG (*A*) and TolB-Pal (*B*) interactions serve as positive controls. *C*, Co-immunoprecipitation assays. Detergent-solubilized extracts of *E. coli* cells producing the indicated VSV-G- and FLAG-tagged proteins were subjected to immunoprecipitation with anti-FLAG-coupled beads. The input (total soluble material, T) and the immunoprecipitated material (IP) were loaded on a 12.5%-acrylamide SDS-PAGE, and immunodetected with anti-FLAG and anti-VSV-G monoclonal antibodies. The immunodetected proteins and the molecular weight markers are indicated. *D*, Biolayer interferometry: PorM and PorN interact with a K<sub>D</sub> of

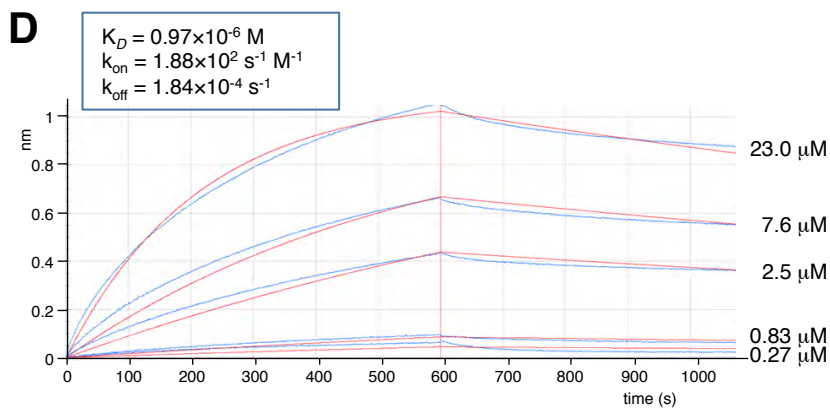
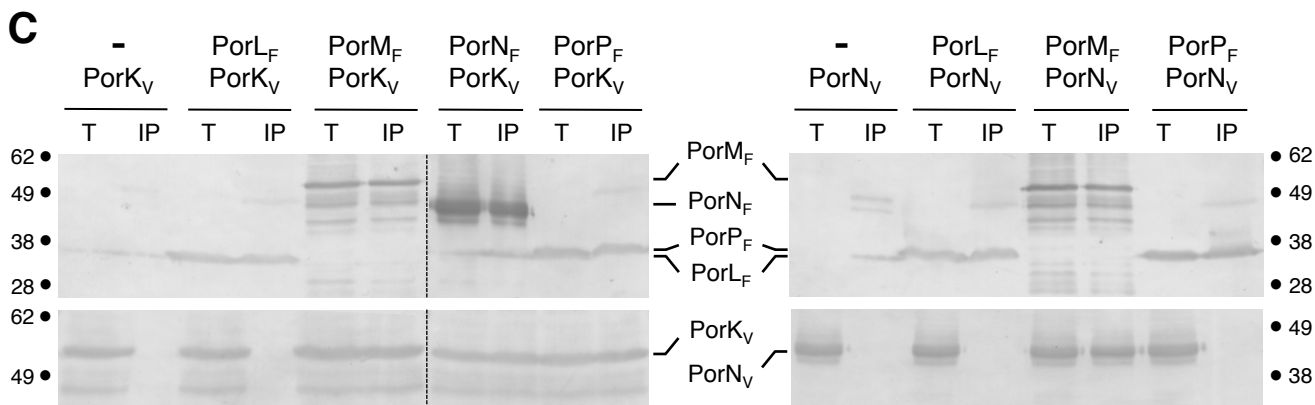
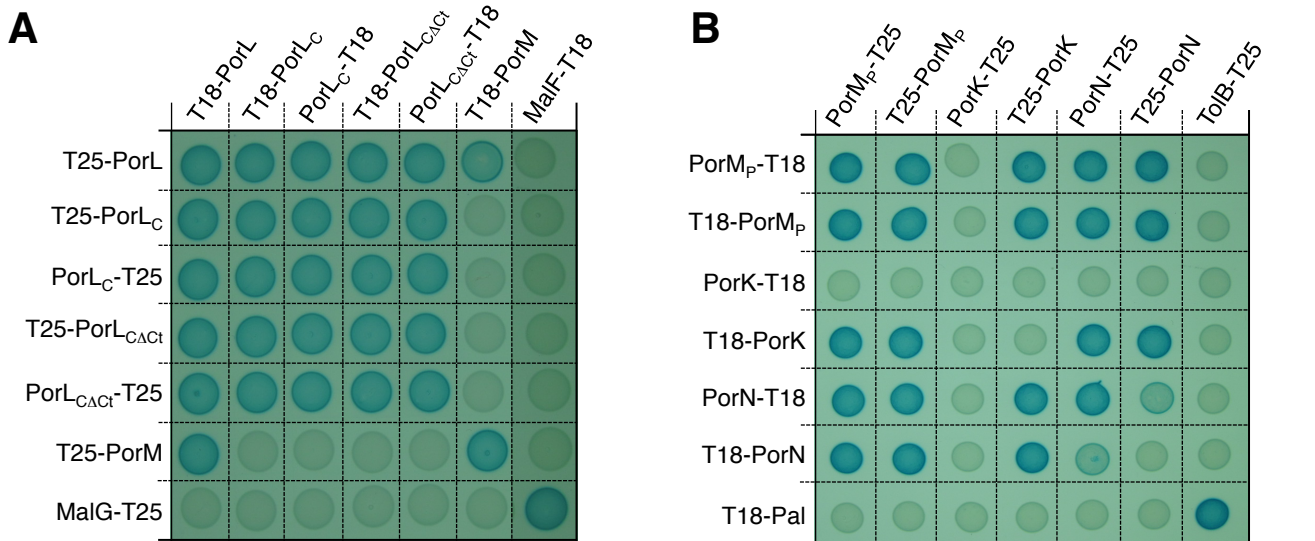
0.97  $\mu\text{M}$ . The recordings represent binding of the indicated concentration of purified  $\text{PorM}_p$  to the sensortip coupled to purified  $\text{PorN}$  (experimental and fitted curves are shown in blue and red respectively). The response (in nm) is plotted versus time (in sec.). The kinetics parameters are indicated in the inset on top.

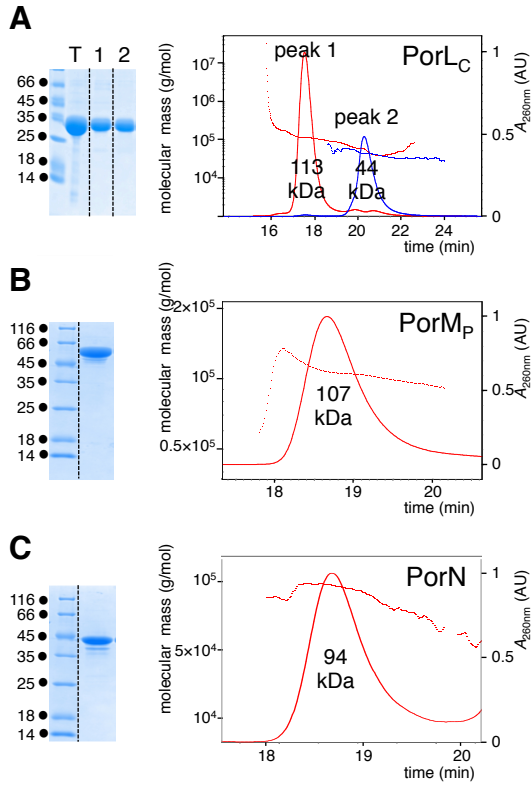
**FIGURE 4. Oligomeric state of the PorL, PorM and PorN soluble domains.** *A-C*, The purified  $\text{PorL}$  cytoplasmic domain ( $\text{PorL}_c$ , *A*),  $\text{PorM}$  periplasmic domain ( $\text{PorM}_p$ , *B*) and the  $\text{PorN}$  protein (*C*) shown in the *left panels* (Coomassie blue staining) were subjected to MALS/QELS/UV/RI analyses (*right panels*). The molecular weights of the proteins or complexes are indicated below their corresponding peaks. The absorbance at  $\lambda=260$  nm (in Absorbance Units, AU) and the molecular mass (in g/mL) are plotted versus the volume of elution (in min).

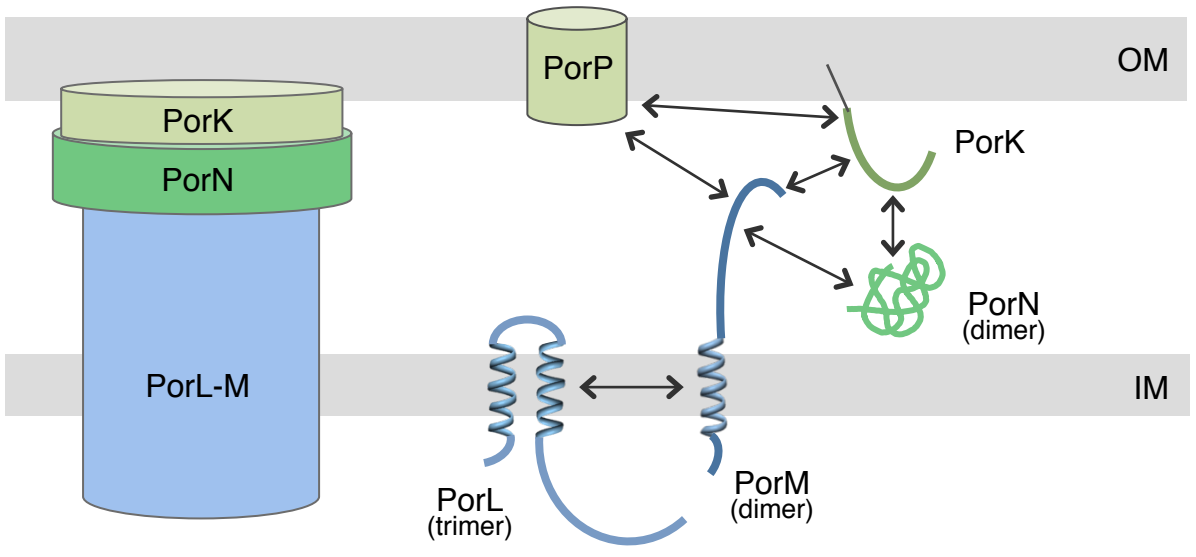
**FIGURE 5. Schematic representation of the PorKLMNP T9SS core complex.** Schematic model of the  $\text{PorKLMNP}$  complex highlighting the localizations and topologies of the proteins, as well as the  $\text{PorP}$  model. The interactions defined by bacterial two-hybrid and co-immune precipitation assays are indicated by arrows. The oligomeric states of the proteins determined by gel filtration experiments are indicated in brackets. The outer membrane-associated  $\text{PorKN}$  complex is depicted as a ring-like structure, as recently shown by negative-stain electron microscopy (29).

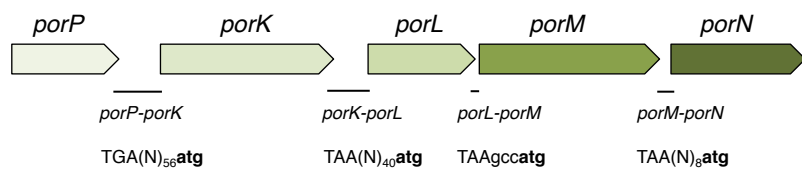
**A****B**

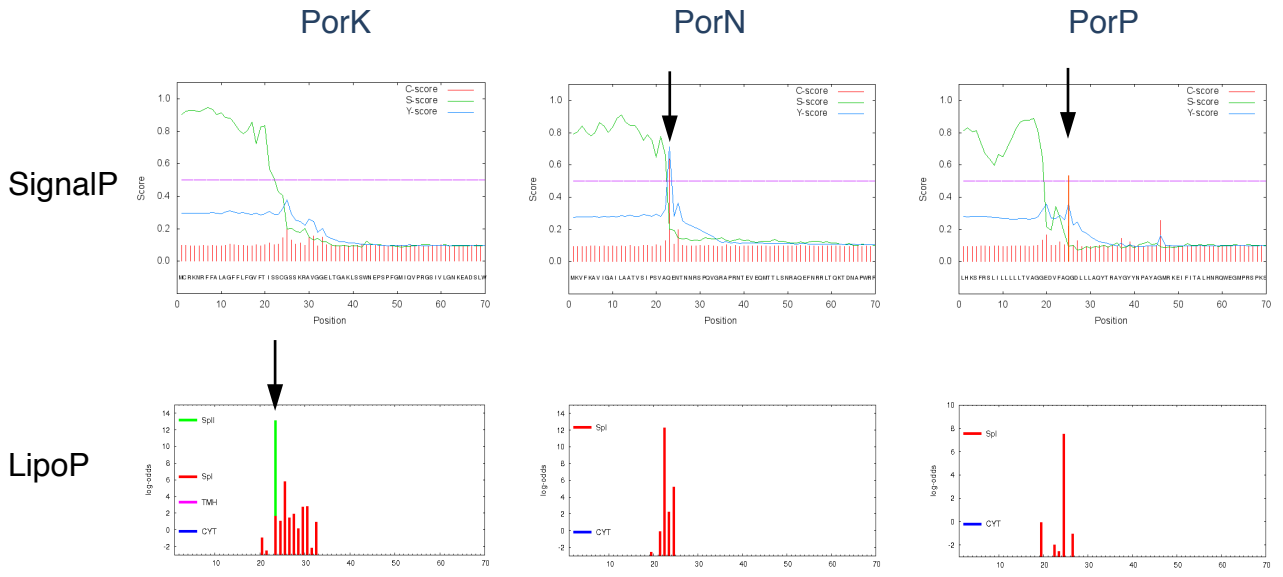


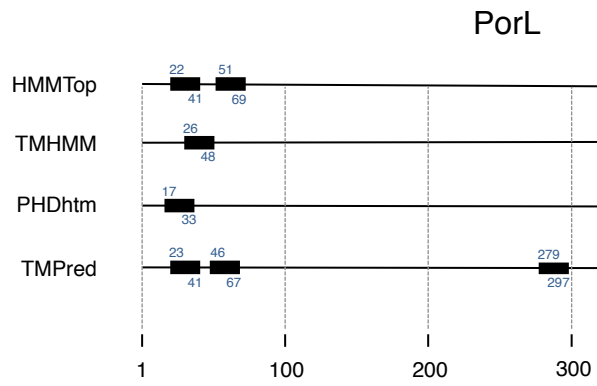
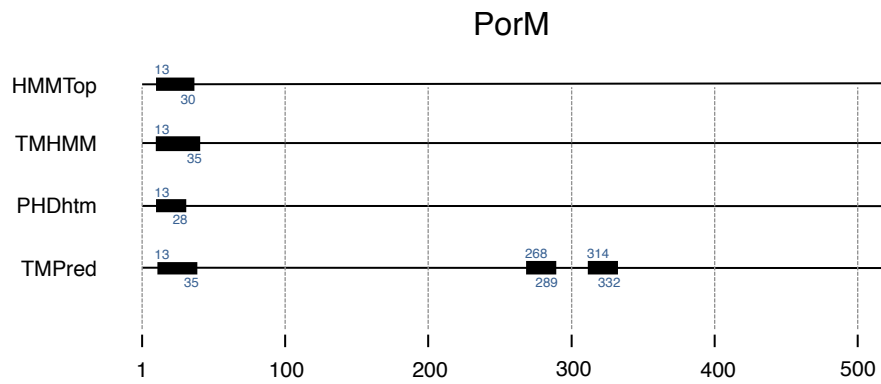


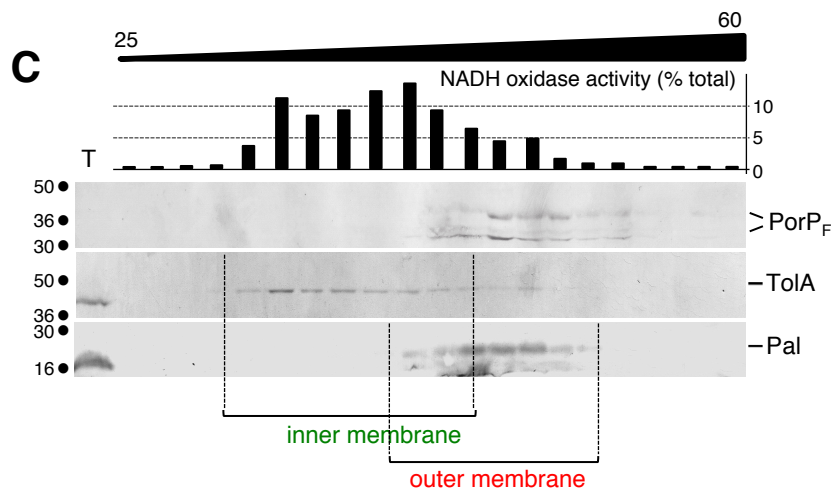
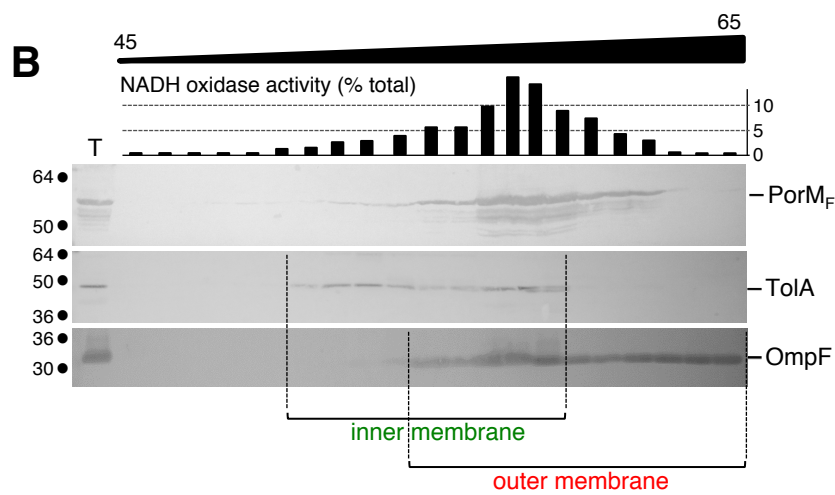
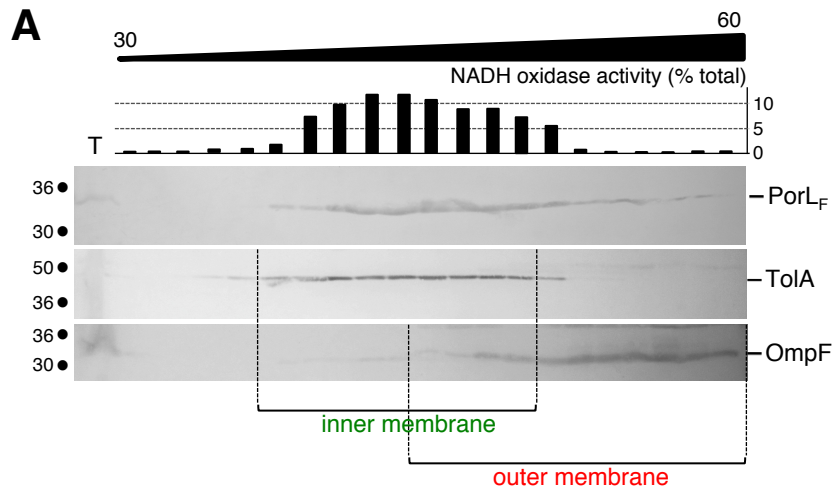








**A****B**



**A**

TMH1
TMH2

---

**PorL** MGHYRRYKNILEMYLASHKGRRL**LLNIVYSWGA****AVVILGALFKLL**HLP-----GNE**MLFVGMITEFLVFFISGF****EKP**AMEY  
**GldL** MALL-----S**KKVMNFAYGMGA**AVVIVGALFKIT**HFEIGPLTGTVM**LSIGLL**TEALIFALS**AF**EP**VEDEL

**B**

TMH

---

**PorM** MAVGSNGNANRQ**KMINLMYL**VFI**AMMALNV**S**SEVL**DGFDKVDKSLTSSIDGSDKRNNLVL  
**GldM** MAGGKL--TPRQ**KMINLMYL**VFI**AMLAMNV**S**KEV**ISAFGLMNEKFEAANTSSVT**TNESLL**

## LEGEND TO SUPPLEMENTAL FIGURES

FIGURE S1. **Genetic organization of the *porPKLMN* locus.** The five genes are indicated in green shades, as well as the sequences of the intergenic regions. Stop codons are indicated in capital letters whereas the start codons of the next genes are indicated in bold letters. The number of nucleotides (N) between stop and start codons is indicated.

FIGURE S2. **Signal sequence analyses.** Computer analyses of the putative signal sequences of the PorK, PorN and PorP proteins using the algorithms SignalP (prediction of Sec-dependent signal sequences and of sites of cleavage by the Signal peptidase I (red bars)) and LipoP (prediction of lipobox motifs and of sites of cleavage by the Signal peptidase I (red bars) and II (green bars)). The most significant results are indicated by arrows.

FIGURE S3. **Trans-membrane helix predictions.** Computer analyses of the putative TMHs of the PorL (A) and PorM (B) inner membrane proteins. The TMHs predicted using the algorithms listed on the left are represented by black rectangles with their start and end positions indicated in blue.

FIGURE S4. **Discontinuous sucrose gradients.** Total membranes (T) from *E. coli* cells producing FLAG-tagged PorL (A), PorM (B) or PorP (C) were separated on a discontinuous sedimentation sucrose gradient. The collected fractions were analyzed for contents using anti-OmpF/anti-Pal (outer membrane, lower panel), anti-TolA (inner membrane, middle panel) and anti-FLAG (upper panel) antibodies and with a NADH oxidase (inner membrane) activity test (upper graph). The positions of the inner and outer membrane-containing fractions are indicated. Molecular weight markers are indicated on the left of each panel.

FIGURE S5. **Trans-membrane sequences of the PorL and PorM proteins.** N-terminal sequences of the *P. gingivalis* PorL (A) and PorM (B) proteins and their *F. johnsoniae* GldL and GldM homologues, highlighting the TMH sequences defined in this study (in bold red) and conserved glutamate residues (in bold green).

TABLE S1. **Strains, Plasmids and Oligonucleotides used in this study.**

**SUPPLEMENTAL TABLE S1. Strains, plasmids and oligonucleotides used in this study.**

## STRAINS

Strains	Description and genotype	Source
<i>Porphyromonas gingivalis</i>		
DSM20709	WT <i>Porphyromonas gingivalis</i> (ATCC33277/DSM20709)	DSMZ collection
<i>Escherichia coli</i> K12		
DH5 $\alpha$	F-, $\Delta$ ( <i>argF-lac</i> )U169, <i>phoA</i> , <i>supE44</i> , $\Delta$ ( <i>lacZ</i> )M15, <i>relA</i> , <i>endA</i> , <i>thi</i> , <i>hsdR</i>	Laboratory collection
W3110	F-, lambda-IN( <i>rrnD-rrnE</i> )1 <i>rph-1</i>	Laboratory collection
BTH101	F-, <i>cya99</i> , <i>araD139</i> , <i>galE15</i> , <i>gakK16</i> , <i>rpsL</i> , <i>hsdR</i> , <i>mcrAB</i>	(Karimova et al., 1998)
Rosetta(DE3)pLys	F-, <i>ompT hsdS gal dcm</i> ( $\lambda$ DE3) pRARE (Cam <sup>R</sup> )	Novagen

## PLASMIDS

Plasmid	Description and main characteristics	Source
Expression vectors		
pASK-IBA37(+)	Expression vector, AHT-inducible, Amp <sup>R</sup>	IBA technology
pIBA-PorL <sub>FLAG</sub>	<i>P. gingivalis porL</i> gene cloned into pASK-IBA37(+), N-terminal FLAG epitope	This study
pIBA-PorM <sub>FLAG</sub>	<i>P. gingivalis porM</i> gene cloned into pASK-IBA37(+), N-terminal FLAG epitope	This study
pIBA-PorN <sub>FLAG</sub>	<i>P. gingivalis porN</i> gene cloned into pASK-IBA37(+), C-terminal FLAG epitope	This study
pASK-IBA4	Expression vector, AHT-inducible, OmpA signal sequence, Amp <sup>R</sup>	IBA technology

pIBA4-PorK <sub>FLAG</sub>	<i>P. gingivalis</i> <i>porK</i> without signal sequence cloned into pASK-IBA4 C-terminal FLAG epitope	This study
pIBA-PorM <sub>PFLAG</sub>	<i>P. gingivalis</i> <i>porM</i> periplasmic domain (aa 36-516) cloned into pASK-IBA4, N-terminal FLAG epitope	This study
pBAD33	Expression vector, L-arabinose-inducible, Cat <sup>R</sup>	(Guzman and Beckwith, 1995)
pBAD-PorK <sub>VSVG</sub>	<i>P. gingivalis</i> <i>porK</i> gene cloned into pBAD33, N-terminal VSV-G epitope	This study
pBAD-PorL <sub>VSVG</sub>	<i>P. gingivalis</i> <i>porL</i> gene cloned into pBAD33, N-terminal VSV-G epitope	This study
pBAD-PorN <sub>VSVG</sub>	<i>P. gingivalis</i> <i>porN</i> gene cloned into pBAD33, N-terminal VSV-G epitope	This study

### Bacterial Two-Hybrid (BACTH)

pUT18	BACTH vector, ColE1 origin, <i>Plac</i> , T18 domain of <i>Bordetella</i> adenylate cyclase, Amp <sup>R</sup> ,	(Karimova et al., 1998)
pUT18C	BACTH vector, ColE1 origin, <i>Plac</i> , T18 domain of <i>Bordetella</i> adenylate cyclase, Amp <sup>R</sup> ,	(Karimova et al., 1998)
pKT25	BACTH vector, P15A origin, <i>Plac</i> , T25 domain of <i>Bordetella</i> adenylate cyclase, Kan <sup>R</sup>	(Karimova et al., 1998)
pKTN25	BACTH vector, P15A origin, <i>Plac</i> , T25 domain of <i>Bordetella</i> adenylate cyclase, Kan <sup>R</sup>	(Karimova et al., 1998)
pT18-PorK	<i>P. gingivalis</i> <i>porK</i> without signal sequence, cloned downstream T18 into pUT18C	This study
pPorK-T18	<i>P. gingivalis</i> <i>porK</i> without signal sequence, cloned upstream T18 into pUT18	This study
pT18-PorL	<i>P. gingivalis</i> <i>porL</i> cloned downstream T18 into pUT18C	This study
pT18-PorL <sub>C</sub>	<i>P. gingivalis</i> <i>porL</i> cytoplasmic domain (amino-acids 73-309), cloned downstream T18 into pUT18C	This study
pPorL <sub>C</sub> -T18	<i>P. gingivalis</i> <i>porL</i> cytoplasmic domain (amino-acids 73-309), cloned upstream T18 into pUT18	This study
pT18-PorL <sub>CΔCt</sub>	<i>P. gingivalis</i> <i>porL</i> cytoplasmic domain without C-terminal hydrophobic region (amino-acids 73-274), cloned downstream T18 into pUT18C	This study
pPorL <sub>CΔCt</sub> -T18	<i>P. gingivalis</i> <i>porL</i> cytoplasmic domain without C-terminal hydrophobic region (amino-acids 73-274), cloned upstream T18 into pUT18	This study
pT18-PorM	<i>P. gingivalis</i> <i>porM</i> cloned downstream T18 into pUT18C	This study
pT18-PorM <sub>p</sub>	<i>P. gingivalis</i> <i>porM</i> periplasmic domain (amino-acids 36-516) cloned downstream T18 into pUT18C	This study
pPorM <sub>p</sub> -T18	<i>P. gingivalis</i> <i>porM</i> periplasmic domain (amino-acids 36-516) cloned upstream T18 into pUT18	This study
pT18-PorN	<i>P. gingivalis</i> <i>porN</i> without signal sequence, cloned downstream T18 into pUT18C	This study
pPorN-T18	<i>P. gingivalis</i> <i>porN</i> without signal sequence, cloned upstream T18 into pUT18	This study
pT25-PorK	<i>P. gingivalis</i> <i>porK</i> without signal sequence, cloned downstream T25 into pKTN25	This study
pPorK-T25	<i>P. gingivalis</i> <i>porK</i> without signal sequence, cloned upstream T25 into pKT25	This study
pT25-PorL	<i>P. gingivalis</i> <i>porL</i> cloned downstream T25 into pKTN25	This study
pT25-PorL <sub>C</sub>	<i>P. gingivalis</i> <i>porL</i> cytoplasmic domain (amino-acids 73-309), cloned downstream T25 into pKTN25	This study
pPorL <sub>C</sub> -T25	<i>P. gingivalis</i> <i>porL</i> cytoplasmic domain (amino-acids 73-309), cloned upstream T25 into pKT25	This study
pT25-PorL <sub>CΔCt</sub>	<i>P. gingivalis</i> <i>porL</i> cytoplasmic domain without C-terminal hydrophobic region (amino-acids 73-274), cloned downstream T25 into pKTN25	This study

pPorL <sub>CAC1</sub> -T25	<i>P. gingivalis porL</i> cytoplasmic domain without C-terminal hydrophobic region (amino-acids 73-274), cloned upstream T25 into pKT25	This study
pT25-PorM	<i>P. gingivalis porM</i> cloned downstream T25 into pKTN25	This study
pT25-PorM <sub>p</sub>	<i>P. gingivalis porM</i> periplasmic domain (amino-acids 36-516) cloned downstream T25 into pKTN25	This study
pPorM <sub>p</sub> -T25	<i>P. gingivalis porM</i> periplasmic domain (amino-acids 36-516) cloned upstream T25 into pKT25	This study
pT25-PorN	<i>P. gingivalis porN</i> without signal sequence, cloned downstream T25 into pKTN25	This study
pPorN-T25	<i>P. gingivalis porN</i> without signal sequence, cloned upstream T25 into pKT25	This study
pTolB-T25	<i>E. coli tolB</i> without signal sequence, cloned upstream T25 into pKT25	Battesti and Bouveret, 2007
pT18-Pal	<i>E. coli pal</i> without signal sequence, cloned downstream T18 into pUT18C	Battesti and Bouveret, 2007
pT25-MalF	<i>E. coli malF</i> cloned downstream T258 into pKTN25	Karimova et al., 2005
pT18-MalG	<i>E. coli malG</i> cloned downstream T18 into pUT18C	Karimova et al., 2005

### Protein purification

pLIC03	pETG28+ derivative, Cole1 origin, PT7 promoter, N-terminal 6×His-TEV, Amp <sup>R</sup>	Novagen
pLIC-PorL <sub>C</sub>	<i>P. gingivalis porL</i> cytoplasmic domain (amino-acids 73-309), cloned into pLIC03	This study
pLIC-PorM <sub>p</sub>	<i>P. gingivalis porM</i> periplasmic domain (amino-acids 36-516) cloned into pLIC03	This study
pLIC-PorN	<i>P. gingivalis porN</i> without signal sequence, cloned into pLIC03	This study

### PorL and PorM substitution variants

pIBA-PorL-S17C	Ser-17 to Cys substitution introduced into pIBA-PorL <sub>FLAG</sub>	This study
pIBA-PorL-M48C	Met-48 to Cys substitution introduced into pIBA-PorL <sub>FLAG</sub>	This study
pIBA-PorL-M74C	Met-74 to Cys substitution introduced into pIBA-PorL <sub>FLAG</sub>	This study
pIBA-PorL-V275	Val-275 to Cys substitution introduced into pIBA-PorL <sub>FLAG</sub>	This study
pIBA-PorL-S302C	Ser-302 to Cys substitution introduced into pIBA-PorL <sub>FLAG</sub>	This study
pIBA-PorM-C92S	Cys-92 to Ser substitution introduced into pIBA-PorM <sub>FLAG</sub>	This study
pIBA-PorM-A9C	Ala-9 to Cys substitution introduced into pIBA-PorM-C92S	This study
pIBA-PorM-V41C	Val-41 to Cys substitution introduced into pIBA-PorM-C92S	This study
pIBA-PorM-S309C	Ser-309 to Cys substitution introduced into pIBA-PorM-C92S	This study
pIBA-PorM-A498C	Ala-498 to Cys substitution introduced into pIBA-PorM-C92S	This study

## OLIGONUCLEOTIDES

Oligonucleotide	Sequence (5' to 3')
<b>Expression vectors<sup>a,b,c,d</sup></b>	
5-pIBA4-PorK	GCAGTGGCACTGGCTGGTTTTCGCTACCGTACTCCTATCTGGGTGCGGCTCTTCCAAACGGGCTGTTG
3-pIBA4-PorK-FLAG	GGTGGCTCCAGCTAGCGGCTGCGCTTATTTATCATCGTCTTTATAATCTTTCTTTATGCTGCGACGCGAACTCTTAGG
5-pBAD-PorK	CTCTCTACTGTTTCTCCATAACCCGTTTTTTTTGGGCTAGCaggaggtattacaccATGAAAAAGACAGCTATCGCGATTGCAGTGG
3-pBAD-PorK-VSVG	GGTCGACTCTAGAGGATCCCCGGGTACCTTATTTTCCTAATCTATTCAATTTCAATATCTGTATAATTTCTTTATGCTGCGACGCG AACTCTTAGG
5-pBAD-PorL-VSVG	CTCTCTACTGTTTCTCCATAACCCGTTTTTTTTGGGCTAGCaggaggtattacaccATGTATACAGATATTGAAATGAATAGATTAGGAA AAGGTCATTATAGAAGATACAAGAACATCCTTGAG
3-pBAD-PorL	GGTCGACTCTAGAGGATCCCCGGGTACCTTATAAGGGTGAGCTGCCGGATGATGAAG
5-pIBA37-PorL-FLAG	GACAAAAATCTAGAAATAATTTTGTTTAACTTTAAGAAGGAGATATACAAATGGATTATAAAGATGACGATGACAAGGGTC ATTATAGAAGATACAAGAACATCCTTGAG
3-pIBA37-PorL	GATGGTGATGGTGATGCGATCCTCTGCTAGCTTATAAGGGTGAGCTGCCGGATGATGAAG
5-pBAD-PorM-VSVG	CTCTCTACTGTTTCTCCATAACCCGTTTTTTTTGGGCTAGCaggaggtattacaccATGTATACAGATATTGAAATGAATAGATTAGGAA AAGCAGTAGGTTCTAATGGGAATGCCAATAG
3-pBAD-PorM	GGTCGACTCTAGAGGATCCCCGGGTACCTTAGTTCACAATTACTTCAATGGCCGGAATCTTAC
5-pIBA37-PorM-FLAG	GACAAAAATCTAGAAATAATTTTGTTTAACTTTAAGAAGGAGATATACAAATGGATTATAAAGATGACGATGACAAGGCA GTAGGTTCTAATGGGAATGCCAATAG
3-pIBA37-PorM	GATGGTGATGGTGATGCGATCCTCTGCTAGCTTAGTTCACAATTACTTCAATGGCCGGAATCTTAC
5-pBAD-PorN	CTCTCTACTGTTTCTCCATAACCCGTTTTTTTTGGGCTAGCaggaggtattacaccATGAAAGTATTCAAAGCAGTCATAGGAGCGATCC
3-pBAD-PorN-VSVG	GTCGACTCTAGAGGATCCCCGGGTACCTTATTTTCCTAATCTATTCAATTTCAATATCTGTATACTTGCGGCGACGAACCGAGC
5-pIBA37-PorN	GACAAAAATCTAGAAATAATTTTGTTTAACTTTAAGAAGGAGATATACAAATGAAAGTATTCAAAGCAGTCATAGGAGCGATC
3-pIBA37-PorN-FLAG	GATGGTGATGGTGATGCGATCCTCTGCTAGCTTATTTATCATCGTCTTTATAATCCTTGCGGCGACGAACCGAGCG
<b>Bacterial Two-Hybrid (BACTH)<sup>b,e</sup></b>	
5-BACTH-PorK	GAAGTCTAGATTGCGGCTCTTCCAAACGGGCTGTTG
3-BACTH-PorK	GAAGGGTACCCCTTTCTTTATGCTGCGACGCGAACTCTTAGG
5-BACTH-PorL-FL	GAAGTCTAGATGGTCATTATAGAAGATACAAGAACATCCTTGAG

5-BACTH-PorL	GAAGTCTAGATGCAATGGAATATCACTGGGAAGAGGTCTTC
3-BACTH-PorL1	GAAGGGTACCCCTAAGGGTGAGCTGCCGGATGATGAAG
3-BACTH-PorL-ΔCt	GAAGGGTACCCCTCGTTGAGTTGGGTCAGTTGGCG
5-BACTH-PorM-FL	GAAGTCTAGATGCAGTAGGTTCTAATGGGAATGCCAATAG
5-BACTH-PorM-TMS	GAAGTCTAGATGATGGTTTCGACAAAGTGGATAAGAGCTTAAC
3-BACTH-PorM	GAAGGGTACCCGTTACAATTACTTCAATGGCCGGAATCTTAC
5-BACTH-PorN	GAAGTCTAGATCAGGAAAATACGAACAACCGCTCTCCG
3-BACTH-PorN	GAAGGGTACCCCTTGCGGCGACGAACCGAGCG

#### Protein purification <sup>b</sup>

5-pLIC03-PorL <sub>C</sub>	CCGAGAACCTGTACTTCCAATCAGCAATGGAATATCACTGGGAAG
3-pLIC03-PorL <sub>C</sub>	CGGAGCTCGAATTCGGATCCTTATTATAAGGGTGAGCTGCCGGATG
5-pLIC03-PorM <sub>p</sub>	CCGAGAACCTGTACTTCCAATCAGATGGTTTCGACAAAGTGGATAAG
3-pLIC03-PorM <sub>p</sub>	CGGAGCTCGAATTCGGATCCTTATTAGTTCACAATTACTTCAATGGC
5-pLIC03-PorN	CCGAGAACCTGTACTTCCAATCACAGGAAAATACGAACAACCGCTC
3-pLIC03-PorN	CGGAGCTCGAATTCGGATCCTTATTACTTGCGGCGACGAACCG

#### Site-directed mutagenesis <sup>f</sup>

A-PorL-S17C	CTTGAGATGTATTTGGCA <b>TGCC</b> CACAAAGGACGCCG
B-PorL-S17C	CGGCGTCCTTTGTGGCA <b>TGCC</b> AAATACATCTCAAG
A-PorL-M48C	GTTGCTCCATTTGCCG <b>TGCG</b> GCAATGAGATGCTTTTC
B-PorL-M48C	GAAAAGCATCTCATTGCC <b>GCA</b> CGGCAAATGGAGCAAC
A-PorL-M74C	GTTTTGAAAAACCCGCAT <b>TGCG</b> AATATCACTGGGAAGAG
B-PorL-M74C	CTCTTCCCAGTGATATTC <b>GCA</b> TGCGGGTTTTTCAAAC
A-PorL-V275C	CTGACCCAACCAACGAG <b>TGCT</b> ATGCTCGCTTGCTCC
B-PorL-V275C	GGAGCAAGCGAGCATAG <b>CACT</b> CGTTGAGTTGGGTCAG
A-PorL-S302C	GGTGCTTCTAATCCTT <b>GCT</b> CGAGCGGCAGCTCACCC
B-PorL-S302C	GGGTGAGCTGCCGCTCGAG <b>GCA</b> AGGATTAGAAGCACC
A-PorM-C92S	GAGGCTGATTTCGCTCT <b>CA</b> ACCTTTATAGATGATCTG
B-PorM-C92S	CAGATCATCTATAAAGGTT <b>TG</b> AGAGCGAATCAGCCTC
A-PorM-A9C	GTAGGTTCTAATGGGAAT <b>TGCA</b> ATAGGCAAAAGATGATC

B-PorM-A9C	GATCATCTTTTGCCTATTG <b>CA</b> ATTCCCATTAGAACCTAC
A-PorM-V41C	GGATGGTTTCGACAAAT <b>TGCG</b> GATAAGAGCTTAACCTC
B-PorM-V41C	GAGGTTAAGCTCTTATC <b>GCA</b> ATTTGTCGAAACCATCC
A-PorM-S309C	GATTCGTCGTGACTTTGAA <b>TGCG</b> AATACTTCGTTACGGAAC
B-PorM-S309C	GTTCCGTAACGAAGTATTC <b>GCA</b> TTCAAAGTCACGACGAATC
A-PorM-A498C	CTACGTAACAGAAGTAATTT <b>TGCC</b> CGGTCCGGATGGTATC
B-PorM-A498C	GATACCATCCGGACCG <b>GCA</b> AATTACTTCTGTTACGTAG

### RT-PCR <sup>f</sup>

RT-5-PorP	GCTTGGGGATGCAGTTGGGC
RT-3-PorK	CGGGGAACCTGTATCATCCCG
RT-5-PorK	GGTAGTACGCGGTGGTTCGTGG
RT-3-PorL	TTGCTCCATTTGCCGATGGGCAATGAGATGCTTTTC
RT-5-PorL	CTGACCCAACCAACGAGGTGTATGCTCGCTTGCTC
RT-3-PorM	GAGGCTGATTTCGCTCTGTACCTTTATAGATGATCTG
RT-5-PorM	CTCCCCGATCCTCTTCCCTATATCG
RT-3-PorN	CCTGCGCAACGGACGGG

<sup>a</sup> sequence corresponding to the RBS in lower case

<sup>b</sup> sequence for amplification of the gene italicized

<sup>c</sup> FLAG or VSVG tag coding sequence underlined

<sup>d</sup> sequence for site directed mutagenesis of the OmpA signal sequence in bold

<sup>e</sup> Restriction site underlined (XbaI at the 5' end, TCTAGA ; KpnI at the 3' end, GGTACC)

<sup>f</sup> mutagenized codon underlined

<sup>g</sup> nucleotide substitutions in bold